

AD-A039 353

NAVAL POSTGRADUATE SCHOOL MONTEREY CALIF

F/G 8/3

KINEMATICS OF BREAKING WAVES IN THE SURF ZONE: EMPHASIZING ANAL--ETC(U)

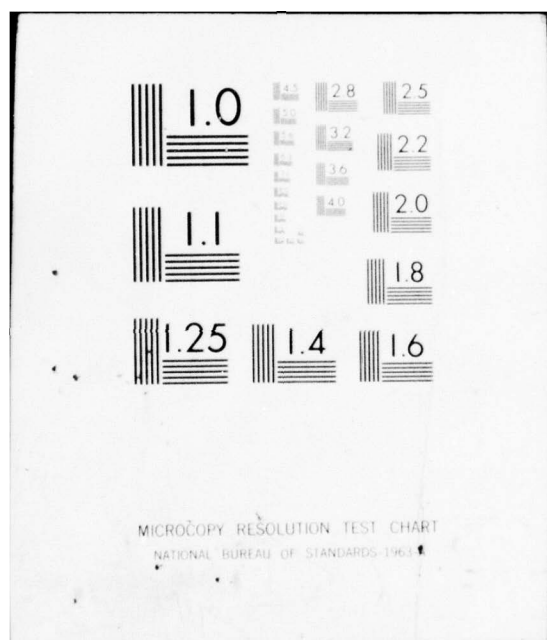
MAR 77 V S HULTSTRAND

UNCLASSIFIED

NL

1 OF 1
AD
A039353





AD A 039353

(2)
NW

NAVAL POSTGRADUATE SCHOOL

Monterey, California



THESIS

KINEMATICS OF BREAKING WAVES
IN THE SURF ZONE: EMPHASIZING ANALYSIS OF
IDENTIFIED AND CLASSIFIED BREAKERS

by

Victor Sandiford Hultstrand

March 1977

Thesis Advisor:

E. B. Thornton

Approved for public release; distribution unlimited.

AD No. _____
DDC FILE COPY



REPORT DOCUMENTATION PAGE		READ INSTRUCTIONS BEFORE COMPLETING FORM
1. REPORT NUMBER	2. GOVT ACCESSION NO.	3. RECIPIENT'S CATALOG NUMBER
4. TITLE (and Subtitle) Kinematics of Breaking Waves in the Surf Zone: Emphasizing Analysis of Identified and Classified Breakers.		5. TYPE OF REPORT & PERIOD COVERED Master's Thesis; Final Report, March 1977
7. AUTHOR(s) 10 Victor Sandiford/Hultstrand		6. PERFORMING ORG. REPORT NUMBER
9. PERFORMING ORGANIZATION NAME AND ADDRESS Naval Postgraduate School Monterey, California 93940		8. CONTRACT OR GRANT NUMBER(s) Office of Naval Research Contract No. NR 388-114
11. CONTROLLING OFFICE NAME AND ADDRESS Naval Postgraduate School Monterey, California 93940		10. PROGRAM ELEMENT, PROJECT, TASK AREA & WORK UNIT NUMBERS
14. MONITORING AGENCY NAME & ADDRESS (if different from Controlling Office) Naval Postgraduate School Monterey, California 93940		12. REPORT DATE 11 March 1977
		13. NUMBER OF PAGES 66 1267p.
		15. SECURITY CLASS. (of this report) Unclassified
		15a. DECLASSIFICATION/DOWNGRADING SCHEDULE
16. DISTRIBUTION STATEMENT (of this Report) Approved for public release; distribution unlimited.		
17. DISTRIBUTION STATEMENT (of the abstract entered in Block 20, if different from Report)		
18. SUPPLEMENTARY NOTES		
19. KEY WORDS (Continue on reverse side if necessary and identify by block number) waves breaking waves surf zone		
20. ABSTRACT (Continue on reverse side if necessary and identify by block number) Measurements were made of the water level fluctuations and horizontal water particle velocities in breaking waves. The breaking waves were identified and classified. The mean value of the height of breaking to depth of breaking was calculated and found to be 0.86 for a composite of the waves measured; the mean ratio values for collapsing, plunging and spilling were 0.84, 0.87 and 0.90, respectively. Probability distributions were plotted for wave heights		

→ and horizontal velocities and qualitatively compared with Rayleigh distributions; the wave distributions fit well but velocity did not. The spectra of wave profile and horizontal velocity were calculated and indicated a narrow banded data set. The coherence values between horizontal water particle velocities and wave profile were generally high, indicating that the horizontal particle velocities measured were highly wave-induced. The phase shift at the peak energy frequency was about 40^{deg} which suggested the presence of reflected waves. ↗

SECTION 101	
NTS	White Section <input checked="" type="checkbox"/>
DC	Buff Section <input type="checkbox"/>
UNANNOUNCED	<input type="checkbox"/>
NOTIFICATION	
DISTRIBUTION/AVAILABILITY CODES	
DISC	ATTN and/or SPECIAL
A	

Kinematics of Breaking Waves
in the Surf Zone: Emphasizing Analysis of
Identified and Classified Breakers

by

Victor Sandiford Hultstrand
Lieutenant, United States Navy
B.S., Mississippi State University, 1968

Submitted in partial fulfillment of the
requirements for the degree of

MASTER OF SCIENCE IN METEOROLOGY AND OCEANOGRAPHY

from the
NAVAL POSTGRADUATE SCHOOL
March 1977

Author

Victor S. Hultstrand

Approved by:

Edward B. Thornton

Thesis Advisor

Joseph Von Schwinde

Second Reader

Dale F. Lipper

Chairman, Department of Oceanography

Robert A. Zimmer

Dean of Science and Engineering

ABSTRACT

Measurements were made of the water level fluctuations and horizontal water particle velocities in breaking waves. The breaking waves were identified and classified. The mean value of the height of breaking to depth of breaking was calculated and found to be 0.86 for a composite of the waves measured; the mean ratio values for collapsing, plunging and spilling were 0.84, 0.87 and 0.90, respectively. Probability distributions were plotted for wave heights and horizontal velocities and qualitatively compared with Rayleigh distributions; the wave distributions fit well but velocity did not. The spectra of wave profile and horizontal velocity were calculated and indicated a narrow banded data set. The coherence values between horizontal water particle velocities and wave profile were generally high, indicating that the horizontal particle velocities measured were highly wave-induced. The phase shift at the peak energy frequency was about 40° which suggested the presence of reflected waves.

TABLE OF CONTENTS

	Page
I. INTRODUCTION - - - - -	12
II. MEASUREMENTS - - - - -	15
A. EXPERIMENT SITE - - - - -	15
B. INSTRUMENTS - - - - -	19
III. ANALYSIS - - - - -	22
IV. RESULTS - - - - -	24
A. SPECTRA - - - - -	24
B. BREAKING WAVES - - - - -	26
C. DEEP WATER WAVES - - - - -	29
D. BREAKING WAVE PARAMETERS - - - - -	33
E. PROBABILITY DISTRIBUTIONS - - - - -	39
V. CONCLUSIONS - - - - -	47
APPENDIX A Wave Gauge Calibration and Flow Meter Calibration - - - - -	49
APPENDIX B Probability Distributions for H_b/h_b , H_b , (+) (-) (-) η_b , V , V , and V_{max}/C_b - - - - -	51
APPENDIX C Field and Calculated Data - - - - -	59
REFERENCES - - - - -	63
INITIAL DISTRIBUTION LIST - - - - -	65

LIST OF TABLES

	Page
I. THEORETICAL BREAKING CRITERIA - - - - -	14
II. BEACH AND WAVE CHARACTERISTICS ON 10 MAY 1976 - - - - -	18

LIST OF DRAWINGS

	Page
1. Figure of Variables for a Wave at the Breaker Position (Galvin, 1968) - - - - -	10
2. Carmel River Beach Experiment Site (4-10 May 1976) - - - - -	16
3. Beach Profile and Instrument Location at Carmel River Beach, 10 May 1976 - - - - -	17
4. Log Spectral Density for Waves and Horizontal Velocities, Phase and Coherence - - - - -	25
5. Plot of Waves and Wave Marker Channel - - - - -	27
6. Illustration of Collapsing Breaker - - - - -	30
7. Reflected Wave Node Relation to Gauge Location - - - - -	34
8. H_b versus h_b for Ocean Breaker Data from the SIO Report of 1949 and This Study - - - - -	36
9. Classification of Present Breaker Types According to Battjes' Reinterpretation of Galvin's Observations - - - - -	38
10. Probability Distribution of Wave Heights and Corresponding Theoretical Rayleigh Distribution - - - - -	40
11. Probability Distribution of Wave Amplitudes and Corresponding Theoretical Rayleigh Distribution - - - - -	41
12. Probability Distribution of Shoreward Horizontal Velocity under a Breaking Wave, Seaward Swash Velocity and Corresponding Theoretical Rayleigh Distribution - - - - -	44
(+)	
13. Probability Distribution of V_{max}/C_b for Collapsing and Plunging Breakers - - - - -	45
14. Probability Distribution of V_{max}/C_b for Composite of All Breakers Measured in This Study - - - - -	46
15. Calibration Curve for the Wave Gauge Used in This Experiment - - - - -	50
16. Probability Distribution of H_b/h_b for Collapsing and Plunging Breakers - - - - -	52

17.	Probability Distribution of H_b/h_b for Composite of All Waves on 10 May 1976	53
18.	Probability Distribution of H_b for Collapsing and Plunging Breakers	54
19.	Probability Distribution of η_b for Collapsing and Plunging Breakers	55
	(+)	
20.	Probability Distribution of V for Collapsing and Plunging Breakers	56
	(-)	
21.	Probability Distribution of V for Collapsing and Plunging Breakers	57
	(-)	
22.	Probability Distribution of V_{max}/C_b for Collapsing and Plunging Breakers	58

TABLE OF SYMBOLS AND ABBREVIATIONS
(All Units are in the M-K-S System)

a	Wave Amplitude
C	Wave Phase Speed
e	Difference Between the Still and Mean Water Level
g	Acceleration of Gravity
T	Wave Period
H	Wave Height (Galvin's Definition)
h	Water Depth Relative to Mean Water Level
K	Shoaling Coefficient
k	Wave Number
η	Elevation of Free Surface Relative to Mean
ρ	Density
L	Wave Length
m	Beach Slope = $\tan \alpha$
σ	Standard Deviation
ξ	Criteria Separating Spilling, Plunging, Collapsing and Surging
t	Time
(+)	
V	Water Particle Velocity Shoreward
(-)	
V	Water Particle Velocity Seaward

Subscripts

b	Value of Quantity at Point Where Breaking Occurs
o	Value of Quantity in Deep Water
i	Initial Value of Quantity
H	Horizontal
Max	Maximum
s	Still Water Level
t	Trough

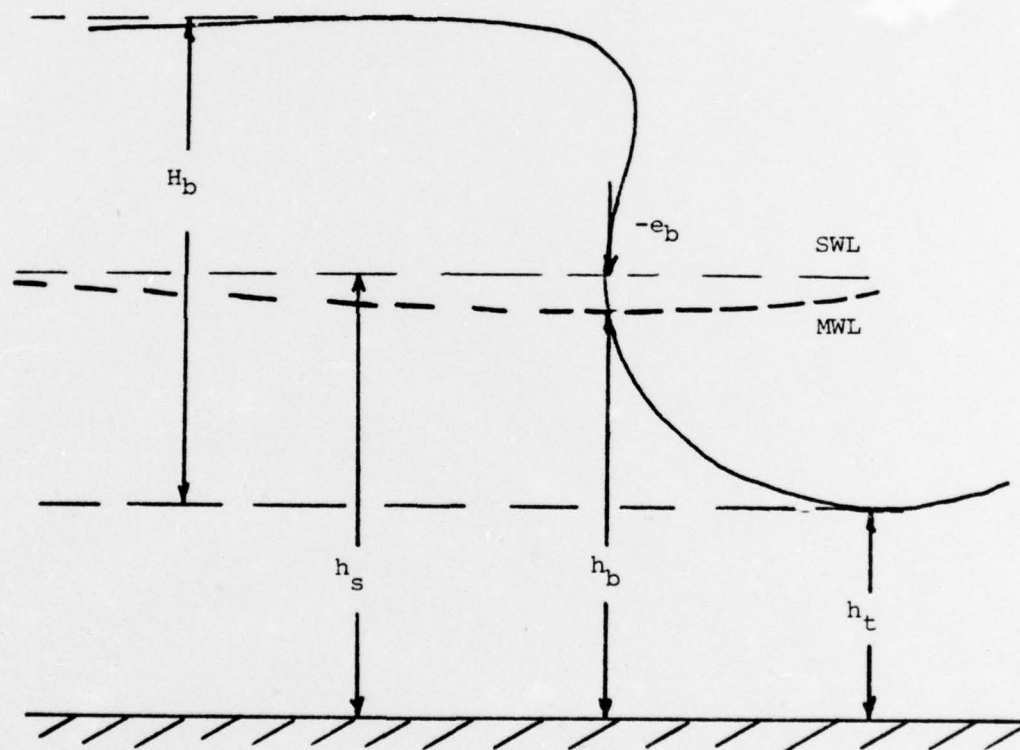


Figure 1. Figure of Variables for a Wave at the Breaker Position (Galvin, 1968).

ACKNOWLEDGEMENTS

First, I would like to express my appreciation to Dr. Edward B. Thornton for his encouragement, patience and assistance during this project. I would also like to thank Mr. Gerry Norton for braving the elements and assisting in placing the measuring equipment. Three very important people behind the successful completion of this thesis are Mr. Edwin Donnellan, Mrs. Kristina Butler and Mr. Manmas Anderson --better known as the Church Computer Center night crew. Their cheerful attitude and bountiful knowledge made an otherwise unpleasant task enjoyable, especially since they started giving gold stars for a job well done.

I. INTRODUCTION

The surf zone is an area bounded on the seaward side by the point where waves first begin to break, and on the landward side by the point of maximum run-up on the beach slope. There are several classifications of breaking waves depending on the wave steepness, water depth, beach slope and wavelength. The most generally accepted classification of breaking waves was proposed by Wiegell (1954), and modified by Galvin (1968). In the Wiegell classification, waves are designated as spilling, plunging and surging. Galvin (1968) found ample evidence to support a fourth class of waves termed "collapsing" (the type that was most often observed during the period that data were being gathered for this thesis).

Spilling waves usually occur over gently sloping bottoms and appear once a wave crest becomes sufficiently unstable to curl over slightly at the peak, with the foamy portion "pouring" down the front slope of the advancing wave form. Plunging waves occur most often on steeper sloping bottoms. This class of breaker is very asymmetrical in form with the top falling all the way down to the base of the wave forming a large sheet splash and subsequent borelike wave front. The collapsing breaker generally occurs on more steeply sloping beaches than spilling breakers. The collapsing type is very similar to the plunging except that it does not break from the highest point of the wave but rather the breaking portion becomes separated from the face of the advancing form at a position somewhat below the peak then falls over in a fashion similar to the plunging type. Another notable difference between the

plunging and the collapsing types is that collapsing breakers occur at the toe of the beach even in the case of very large waves, such as those observed at Carmel River Beach.

The last classification is the surging breaker which is commonly observed on very steeply sloping beaches. The surging breaker builds to a peak but instead of breaking in the usual way it seems to subside under its own weight with the forward divergent momentum forcing the water up the beach slope in a quiet, sudden "surge"; hence the name.

Many investigators have made attempts to define, derive or empirically determine various breaking criteria. Among those who have presented theoretical developments are Boussinesq (1871), Lord Rayleigh (1876), McCowan (1900), Rackham (1952), Davies (1952), Yamada (1957), Lenau (1966), Laitone (1963), Chappellear (1959) and Dean (1968). Of the several breaking criteria proposed there are three main categories; kinematic, dynamic and geometrical. A brief description of the various criteria is given in Table I.

There have not been many precise measurements made of breaking waves and even fewer have been actually made in the field. Most measurements have been made in laboratory wave tanks.

For this thesis breaking wave profiles and the particle velocities beneath them were measured in the field on a very steeply sloping (0.11) beach. The waves varied in height from approximately 0.22 to 0.92 meters.

The objective was to measure probability distributions of H_b and h_b , for breaking waves in the surf zone and the water particle velocities beneath the waves. Measurements were made on a steep beach to ascertain the shape dependence on breaking wave parameters. The ultimate objective of this and related studies is to devise a scheme for predicting the wave height and water depth at breaking.

TABLE I. THEORETICAL BREAKING CRITERIA

KINEMATIC	<p>$V > C_b$, i.e., the limiting value for the water particle velocity at the wave crest is greater than the wave phase speed. If the particle velocity exceeds this value, it would separate itself from the waveform.</p>
DYNAMIC	<p>1) Maximum vertical particle acceleration cannot exceed the gravitational acceleration (ρ constant, surface pressure constant). The water particle leaves the surface vertically for larger accelerations.</p> <p>2) Limiting pressure gradient is zero.</p>
GEOMETRICAL	<p>The surface slope of the wave steepens as the wave shoals. The limiting value for this slope is infinite which is a vertical face. Beyond this, the water particles fall forward ahead of the wave.</p>

II. MEASUREMENTS

A. EXPERIMENT SITE

During the period of 3 May to 12 May 1976 an experiment was conducted at Carmel River Beach in the Monterey, California area (see Figure 2). Four days were spent putting the equipment in place. Because of large wave conditions the task was both arduous and time consuming. Removing the equipment was much easier due to the fact that a hurricane off Baja California produced a large swell and associated breakers, one of which carried away most of the equipment, thus terminating the experiment.

The Carmel River Beach site was chosen for several reasons. First, it is located in an embayment which causes the waves entering the bay to be directionally filtered and refracted by the geometry of the bay so that narrow-banded waves impinge almost perpendicular to the beach. Therefore, in one respect, the description of the waves is greatly simplified.

The second reason for choosing the Carmel River Beach site was to study waves breaking on a steep beach slope. The resulting wave system was not at all simple because of the presence of strongly reflected waves. The steep slope produced breakers primarily of the collapsing type with lesser numbers of spilling, plunging and surging breakers.

Figure 3 shows the beach profile and instrument location at Carmel River Beach on 10 May 1976. Table II gives the characteristics of the beach.

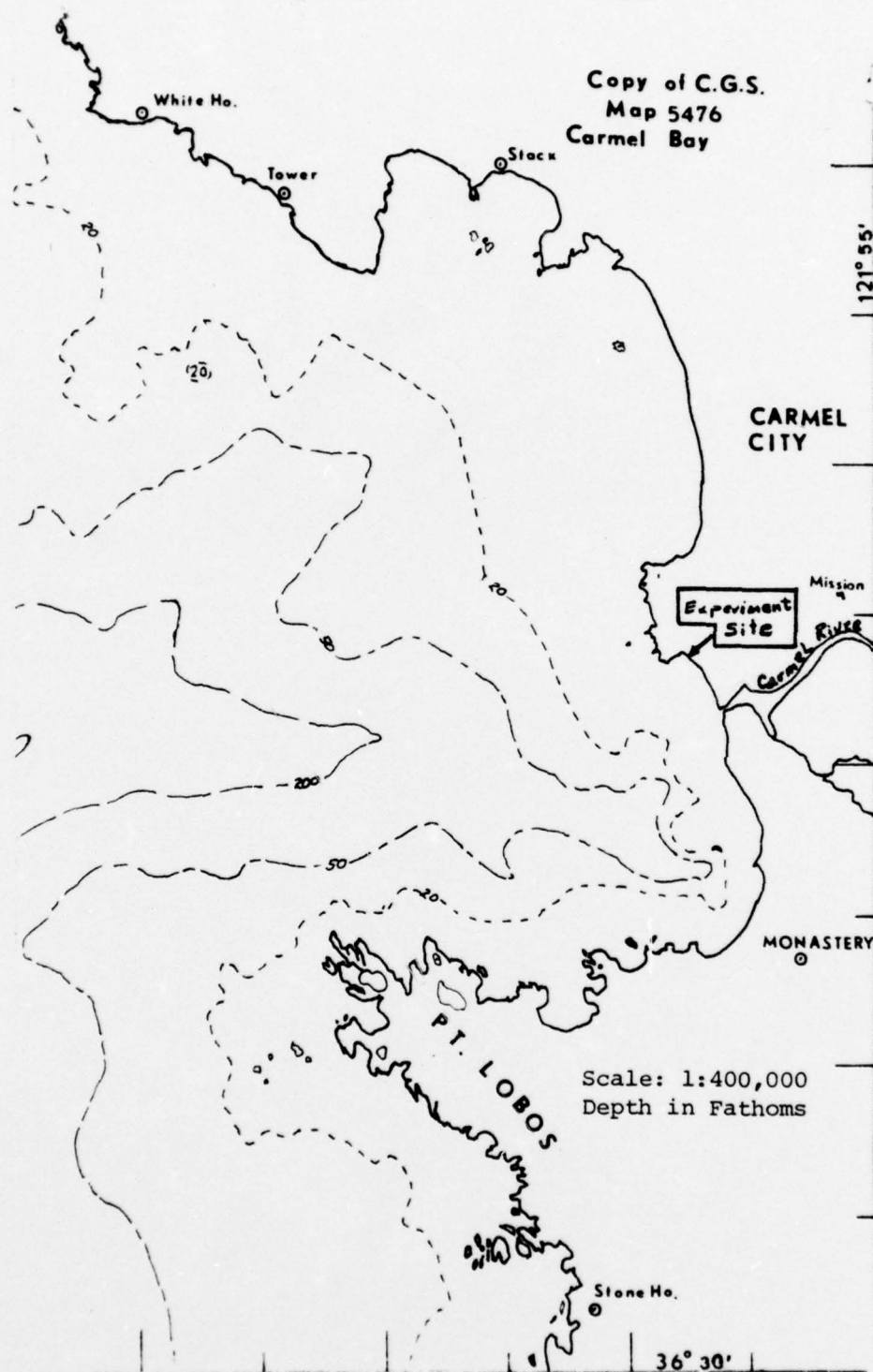


Figure 2. Carmel River Beach Experiment Site (4-10 May 1976).

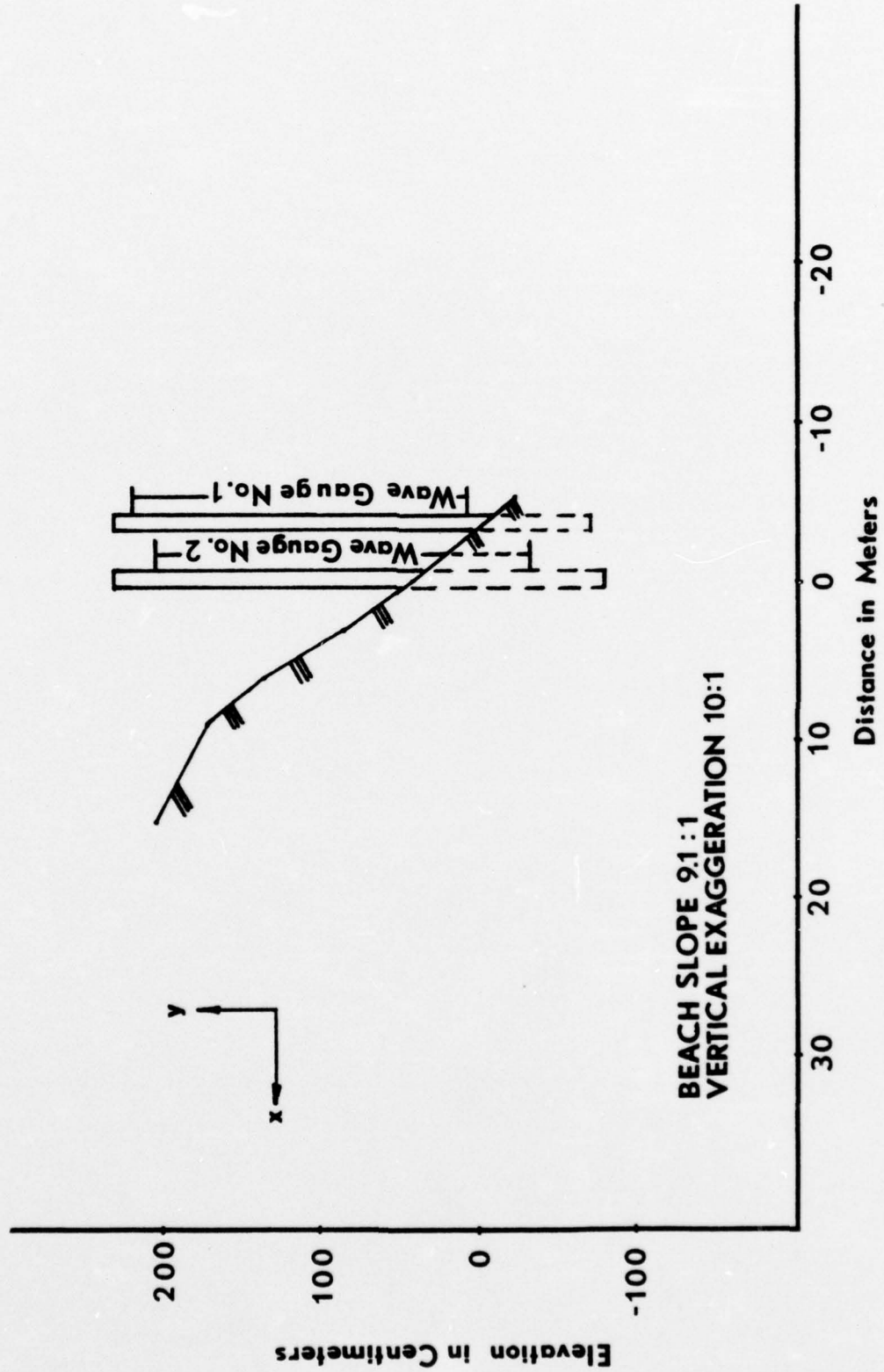


Figure 3 . Beach Profile and Instrument Location at Carmel River Beach
10 May 1976

TABLE II. BEACH AND WAVE CHARACTERISTICS ON 10 MAY 1976

<u>Location:</u>	<u>Carmel River Beach</u>
Beach Slope:	9:1
Sand Composition:	Quartz feldspar
Sand Median Diameter:	0.6 mm (after Bascom, 1946)
Breaker Type:	Collapsing and Plunging
Wave Period:	10.56 seconds
Wave Height:	Up to 3.5 meters

B. INSTRUMENTS

The wave gauges were of the capacitance type constructed of 3/8 inch outside diameter stainless steel rod covered with 1/16 inch wall thickness polypropylene tubing that fit tightly over the rod; these wave gauges proved to be sufficiently sturdy to withstand the severe force of the surf zone. The only real problem that occurred with the gauges was one of water proofing the electrical contacts. The gauges operate on the principle that a change in capacitance is noted as a change in plate dimension occurs. In these gauges the 3/8 inch steel rod and sea water act as the two plates and the polypropylene cover acts as the dielectric. As the water level rises around the gauge, as in a passing wave, there is a change in the capacitance which is sensed by a self-contained battery powered transistorized circuit that produces a linear change in the output voltage. The circuit was designed by McGoldrick (1969) and housed in a watertight container mounted on the support tower.

A static calibration of the wave gauge was accomplished in the laboratory by lowering the gauge into a deep tank. Using the battery powered circuit and short connecting leads to reduce induced capacitance, an accuracy of ± 0.005 meters was established. A plot of voltage output as a function of depth of emersion was plotted and the slope of the curve was used to determine the conversion constant from volts to meters. The calibration plot is shown in Appendix A.

The flow meter used was an EPCO Model 6130 Electromagnetic Ocean Current Meter which works on Faraday's principle of electromagnetic induction. The meter measures water velocity in two orthogonal directions. The flow meter was dynamically calibrated by oscillating it in a water tank. This procedure was used because the characteristics were expected

to be different under rapidly changing flow conditions than those produced by steady flow (see Appendix B). The problems encountered with the flow meters were caused by the extremely harsh conditions to which they were subjected such as abrasion by waterborne sand, gravel and various other forms of debris, including the experimenters themselves when knocked about by the waves.

Two Interstate Electronics Corporation Model SDP 201 pressure transducers were placed in 5.5 meters of water at a distance of 47.5 meters directly seaward of the outermost tower. The pressure sensor is a small, unbonded strain gauge bridge. Direct current excitation for the bridge is supplied by a voltage regulator located in the transducer housing. The sea pressure is coupled by a neoprene diaphragm to a silicone fluid filling the interior. One part of the transducer is exposed directly to the interior fluid and the other is connected to a chamber which is connected to the interior fluid by a length of capillary tubing. This arrangement acts as a hydraulic filter developing a reference pressure which is an average value of the external sea pressure. By the action of this filter the transducer senses rapid pressure fluctuations only and slow changes such as tides are lost through the hydraulic filter. The pressure transducers were put in place by divers, and the signals were cabled to the beach.

The instruments, with the exception of the pressure transducers, were attached to a 3.6 meter high tower constructed of steel pipe with an outside diameter of 6.3 cm. A 1.0 meter diameter base plate was placed about 0.6 meters from the bottom of the tower. This configuration allowed the towers to be sunk approximately 0.65 meters into the sand and provide firm support. The towers were also supported by steel guy wires fastened

to blade anchors driven into the sand. At low tide the first tower was placed as far as possible seaward. The seaward extent was limited only by the ability of the experimenters to wade around in 1 meter of water and sledge an anchor into the bottom while waves of 1 to 1.5 meters broke over their heads. However, after considerable effort the seaward tower was placed. The second tower was located shoreward of the first in a line perpendicular to it.

The capacitance wave gauge, along with a stiffening rod which also acted as the ground lead, was mounted on the outer tower. A specially designed bracket was used to hold the wave gauge 20 cm away from the tower and thus avoid any possible interference between the tower and the gauge. The flow meter was mounted directly below the wave gauge and close to the bottom.

The instruments were tied to the shore facilities by coaxial cables run over the tops of the towers to a support tower on the beach berm. Located at the support tower was a push button switch that actuated a one volt signal generator. The switch was installed so that an operator using a prearranged code could "mark" each wave that broke directly on the wave gauge according to visually estimated breaker type (spilling, plunging, collapsing or surging). The mark in the form of an electrical impulse was recorded and used to categorize breaker type. All signals were recorded using a Vidar Corporation 32-channel digital data acquisition system. An 8-channel Brush strip chart recorder was used for continuous monitoring of the instruments.

III. ANALYSIS

The data collected at Carmel River Beach on 10 May 1976 were selected for analysis. Table II contains the conditions prevailing during the experiment. The data include a record of instantaneous water level, horizontal water particle velocities and identified and classified waves that broke directly on the wave gauge. The digitized wave records were converted to analog records and plotted using an IBM 360 computer in conjunction with a CALCOMP model 765 plotter. A mean water level was computed using a running mean technique. Segments of the total record, each 384 seconds long, were plotted. The reason for this particular record length was to put a maximum number of waves on a minimum number of plots and still preserve visual resolution. Horizontal water particle velocities underneath the waves were plotted in a similar fashion.

The plots were manually analyzed in the following way. First the marked breaking waves were measured for height at breaking. Next the value of depth at breaking was determined and referenced to mean water level, which Galvin (1968) proposed as more reasonable than being referenced to still water level. The ratio of the breaker height to the depth at breaking was computed as was the ratio of horizontal water particle velocity to calculated wave speed at breaking. Probability distributions were calculated for each of the parameters and compared to a Rayleigh distribution. The variances, standard deviations and average values were calculated for each of the parameters.

Spectra, coherence and phase between waves and horizontal velocities were also calculated. The data were sampled every 0.00375 seconds resulting in a Nyquist frequency of 2.0833 Hz. Three 30-minute records were analyzed. Using a maximum lag time of 5% of the record, the bandwidth resolution is 0.00728 Hz. Computing the spectra in this manner results in 40 degrees of freedom for each spectral estimate. The 80% confidence limits for 40 degrees of freedom using a chi-square distribution are between 0.73 and 1.30 of the measured power spectral estimates.

IV. RESULTS

A. SPECTRA

Analysis of the field data (Appendix C) collected at Carmel River Beach on 10 May 1976 showed that of the 398 waves recorded, 59 broke on the gauges and these waves ranged in size from 0.22 meters to 0.92 meters. The point of breaking, or depth at which a wave breaks, is functionally related to the wave height. Since wave height can be considered as a random variable it follows that the point of breaking will tend to be random as well. Because the point of breaking is random, only about 15% of the waves on 10 May 1976 broke directly on the measurement towers. The larger waves that were present were breaking "outside" or seaward of the gauge and those which were of smaller size were breaking "inside" or shoreward of the gauge.

Figure 4 is a plot of the log spectral density of the waves and the horizontal water particle velocity. The plot represents the data from one 30 minute segment of a 90 minute data set recorded at Carmel River Beach on 10 May 1976. The spectrum is narrow banded with the peak energy at 0.0947 Hz, corresponding to a 10.56 second period. There is a second peak in the spectrum approximately half the primary frequency and represents an approximate sub-harmonic of 0.0947 Hz. Guzza and Davis (1974) state that in a theoretical analysis of edge waves excited by incoming waves the prominent edge wave mode is the first sub-harmonic of the primary frequency. Finally, the spectral value at about 0.012 Hz probably represents surf beat which generally falls in the range from 0.01333 Hz to 0.0083 Hz or periods of 75 to 120 seconds.

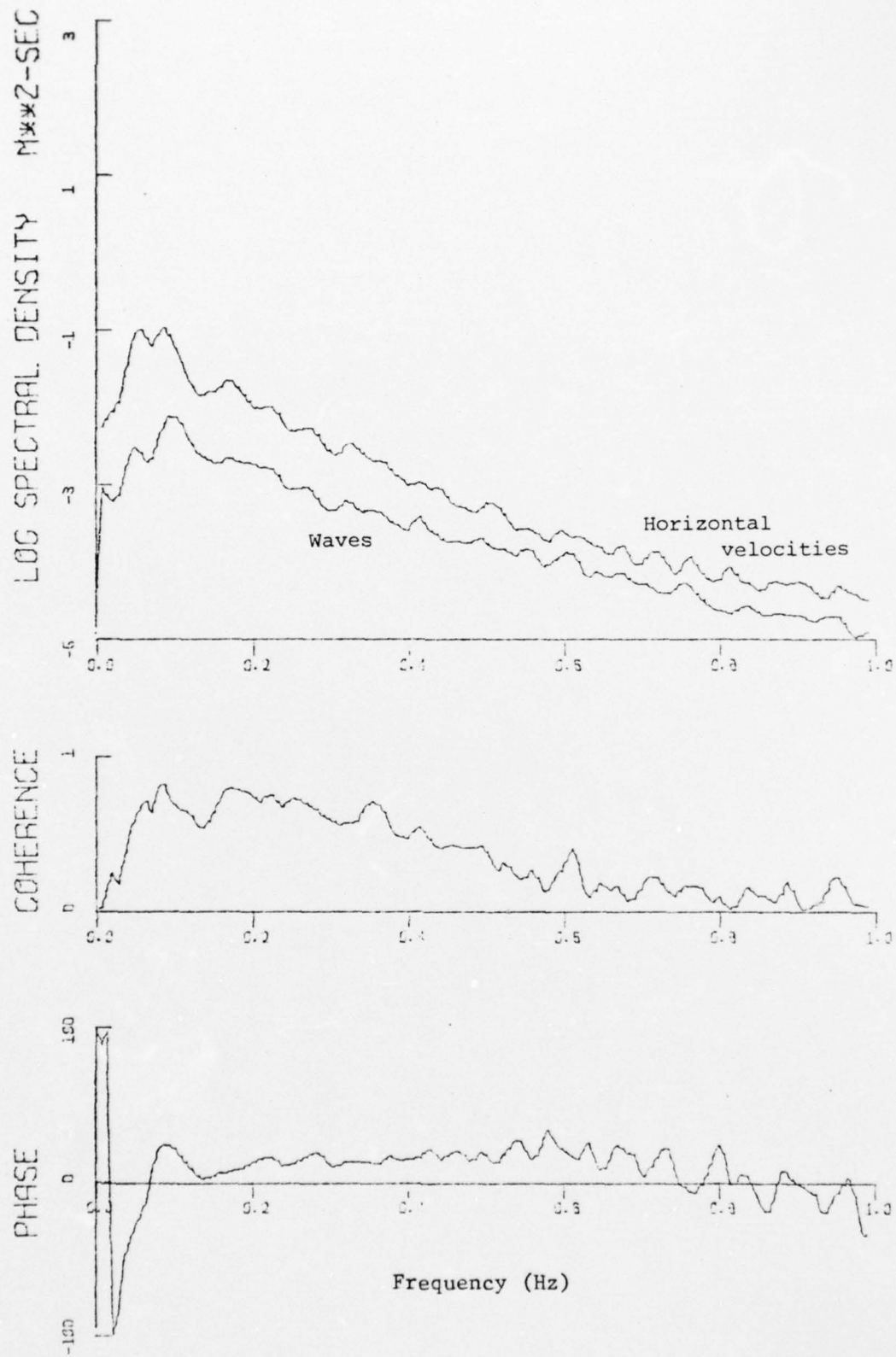


Figure 4. Log Spectral Density for Waves and Horizontal Velocities, Phase and Coherence.

The coherence values between waves and horizontal velocity were moderately high, greater than 0.70 indicating the velocities are primarily wave induced over a frequency range of 0.0510 to 0.2622 Hz. But, for the rest of the frequency range the values are quite small.

The crests of breaking waves tend to lead the horizontal particle velocities in the body of the wave. There was approximately a 40 degree phase lag between the wave crest and the horizontal velocity at the peak frequency. The phase difference between waves and velocities would be expected to be zero for progressive waves. The large value is presumably due to the presence of reflected waves.

B. BREAKING WAVES

The values of the height at breaking were measured directly from the plots of the wave record. Wave record plots produced by the CALCOMP 675 were first matched with plots of the wave marker (Figure 5) and each wave of interest, that is one which broke directly on the tower, was marked. The vertical distance between the maximum and minimum water surface elevations about a zero up-crossing at the breaker point was measured and this value used as the breaker height. This definition of breaker height was in most instances adequate; however, in some cases a problem arose when trying to analyze the record using this definition. The problem manifested itself whenever there were waves in the record that were obviously composed of harmonics or secondary waves, as in the case of wave 33 in Figure 5. Values of the parameters for the total record are presented in Appendix C.

It was found that the mean value of the amplitude of the waves at breaking was a little more than two-thirds of the wave height at breaking, or $\eta_b = 0.68 H_b$. If one considers these values relative to the mean

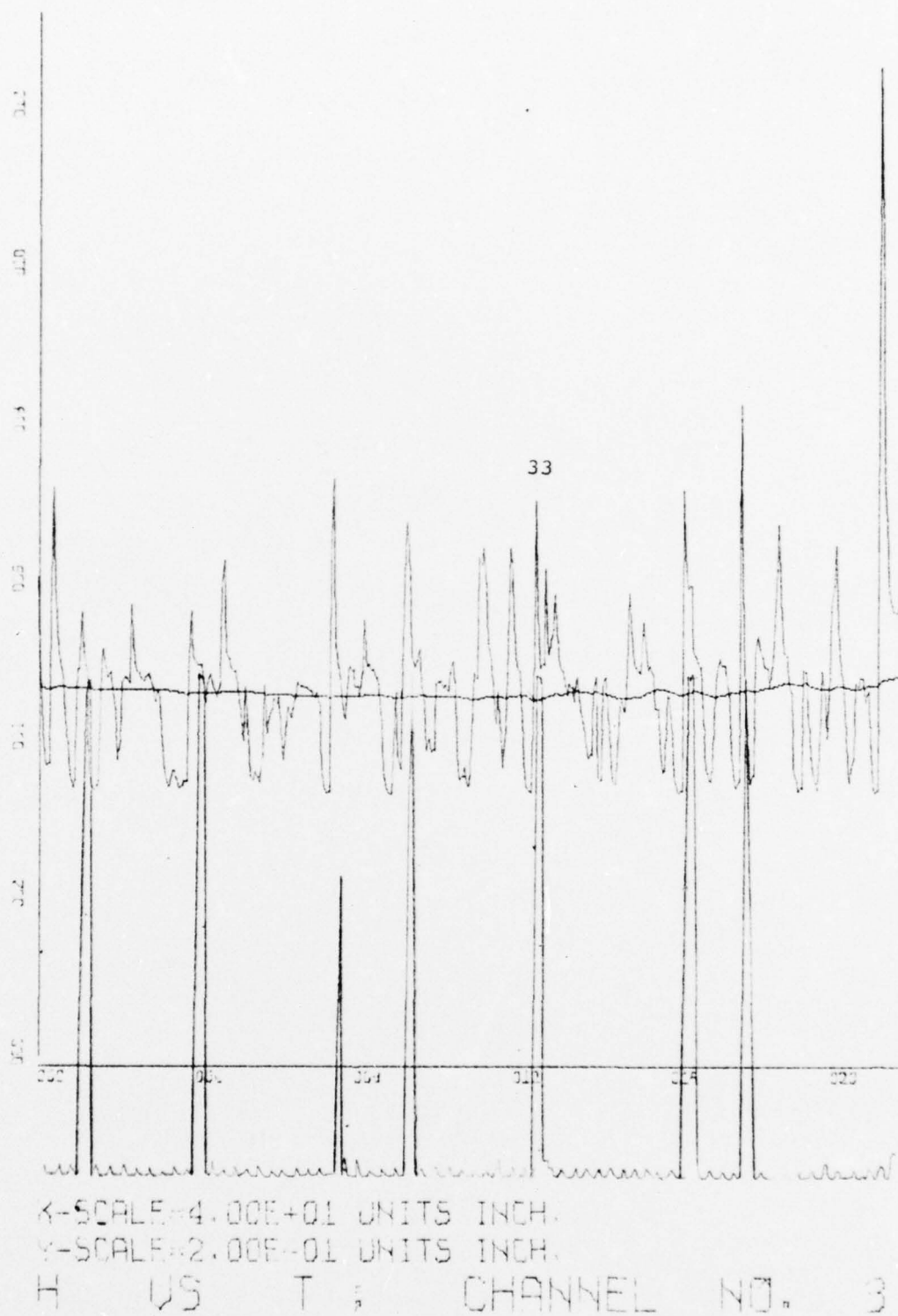


Figure 5. Plot of Waves and Wave Marker Channel.

water level it is seen that the height of the wave crest above mean water level is, in the mean, 1.5 times the depression of the trough below mean water level. The mean value of 1.5 for the crest to trough ratio results from averaging over the whole record; some values were much less but in some extreme cases the ratio was as great as 5.5. There was not enough data to conclusively state that the ratios were much greater for one particular wave type than another although visual observations suggested that the crest to trough ratio was the greatest for collapsing breakers.

The value of the depth of breaking (h_b) was taken to be the depth of the water from the mean water level to the bottom. This value was measured at the point of zero up-crossing following the trough of a wave immediately preceding one of the marked waves. The mean water level was chosen as the reference level in determining the value of h_b because it gives a better representation of the actual water level at any given instant than still water level. The average water level was calculated using a running mean technique averaged over 800 data points, or 24 seconds.

Even the mean water level is not always a particularly good reference for the value of the height of breaking. It was observed that some of the waves actually broke at a point where the water depth in the backwash was almost zero.

Waves shoal rapidly on a steeply sloping beach face. The first and most obvious occurrence is the steepening of the wave from an almost indistinguishable crest line in deeper water to a very definite crest and trough system closer to shore. The wave celerity slows and the leading edge at the base of the trough may even slow to a stop relative to the

backwash running down the beach slope. This supports the idea that the swash can be a dominant factor on steep beaches. At the stationary "foot" of the wave, drawdown and gravity are working together to supply water to the growing "wall" or waveface (see Figure 6); but this is not happening fast enough and therefore a water deficit develops. Turbulence and the resulting trapped air is carried to the base of the building wave and up the face creating voids below the wave crest. Vertically moving water particles also gain forward momentum from the advancing crest, causing them to separate from the wave face before reaching the crest. Thus the wave, lacking support and having forward motion in the upper regions, gives the appearance of a plunging breaker that has had its support removed. As Galvin (1968) pointed out these breaking waves occur at the toe of the beach, or the lowest reach of the backwash. The toe of the beach is the only place that this can occur since a water deficit is necessary to have a collapsing breaker.

This phenomenon does not show up on wave records because a mean reference or still reference is used, which by its very nature, masks short term extremes. Since the collapsing mechanism occurs in the trough region immediately preceding a breaking wave, perhaps the instantaneous water level below the trough should be thought of as the depth of breaking.

C. DEEP WATER WAVES

A mean value of the initial deep water wave height (H_0^i) was calculated from the spectrum of the offshore pressure record. The pressure record was converted to a surface elevation using linear wave theory for which pressure at depth, ΔP , due to the waves is given by

$$\Delta P = \rho g a \frac{\cosh k(h+z)}{\cosh kh} \cos (kx - \sigma t) \quad (1)$$

Wave "collapses" as turbulence
removes support from below

Forward momentum
carries crest over

Swash cannot supply
enough water; turbulence
is carried up wave face

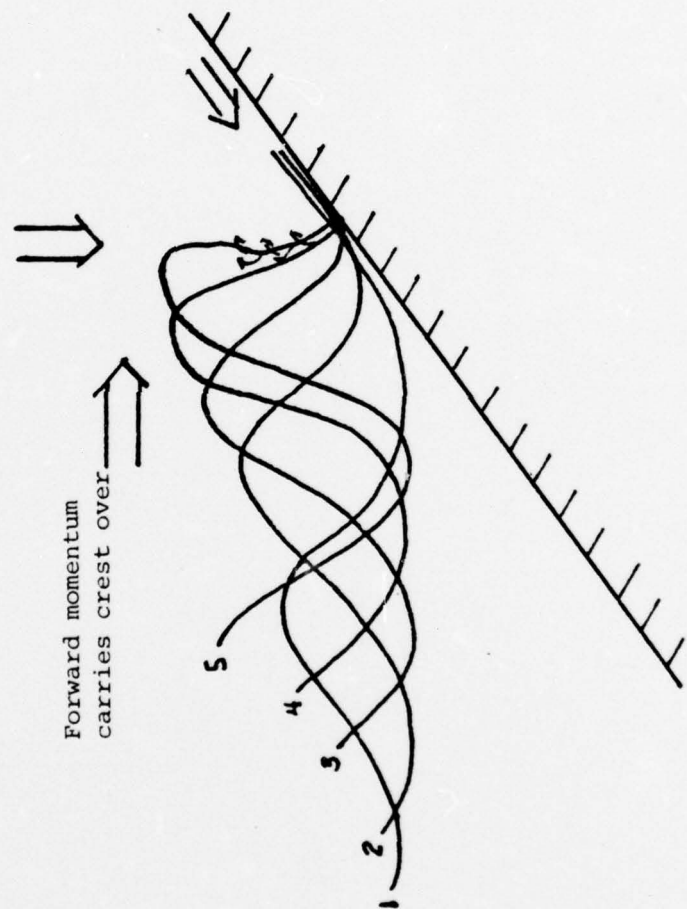


Figure 6. Illustration of Collapsing Breaker.

The wave profile is

$$\eta = a \cos (kx - \sigma t) \quad (2)$$

so that
$$\Delta P = (\rho g \frac{\cosh k(h+z)}{\cosh kh}) \eta \quad (3)$$

The term in the brackets expresses the spectral transfer function $H_1(f)$ relating the surface profile spectrum to the pressure spectrum

$$S_{\eta_1}(f) = |H_1(f)|^2 S_{p_1}(f) \quad (4)$$

The deep water wave amplitude, a_o , can be related to the amplitude at the measurement depth, a_1 . Assuming conservation of energy and applying linear wave theory

$$\frac{1}{2} \rho g a_1^2 c_1 n = \frac{1}{2} \rho g a_o^2 c_o \frac{1}{2}, \quad (5)$$

$$a_o = \left[\frac{K_o}{K_1} \left(1 + \frac{2kh}{\sinh 2kh} \right) \right]^{1/2} a_1 \quad (6)$$

where K_o = initial deep water shoaling coefficient
 K_1 = shoaling coefficient at point of breaking.

The term in the brackets is the spectral transfer function, $H_2(f)$, relating the deep water spectrum to the surface profile spectrum at any depth,

$$S_{\eta_o}(f) = |H_2(f)|^2 S_{\eta_1}(f). \quad (7)$$

The spectral transfer functions can be combined to calculate the deep water wave spectrum from the pressure spectrum, thus

$$S_{\eta_o}(f) = |H_1(f)|^2 |H_2(f)|^2 S_{P_1}(f) \quad (8)$$

The calculated deep water wave spectrum was integrated from 0 to 0.3 Hz to obtain the variance of the wind waves. The variance of the initial deep water waves was found to be $\sigma_{\eta_o}^2 = 0.038 \text{ meters}^2$.

Assuming the wave heights in deep water to have a Rayleigh distribution, the significant wave height can be calculated from the variance

$$H_o'_{1/3} = 4\sqrt{\sigma_{\eta_o}^2} = 0.78 \text{ meters} . \quad (9)$$

Similarly, the mean deep water wave height is given by

$$\bar{H}_o' = 1.77 \sqrt{2\sigma_{\eta_o}^2} = 0.49 \text{ meters} \quad (10)$$

but the mean height at breaking from the data was found to be 0.42 meters, which was less at breaking than in deep water. From theory this should not be the case. As a wave shoals, the wavelength shortens and the height increases while the period remains the same. It was first postulated that reformed waves were being measured resulting in the low breaking wave heights observed, but this idea was rejected. It was decided that reflected waves very likely were the reason for the apparent contradiction.

Reflected waves would be expected to be important since the slope at Carmel River Beach at the time of observation was a very steep 0.11. The data further indicated that the horizontal shoreward velocities are

about the same or somewhat less than the seaward swash velocities. The difference in these velocities could be an effective mechanism in the generation of reflected waves. For a reflected wave off an idealized plane boundary the nodal point is a distance of $L/4$ from the reflecting surface (see Figure 7). The approximate distance from where the mean water level intersects the beach to the measurement tower, x , can be determined from the beach geometry, such that

$$\tan \beta = \frac{\bar{h}}{x} \quad (11)$$

where $\tan \beta$ = beach slope and \bar{h} = mean water depth = 0.49.

Solving, $x = 4.5$ meters.

The wavelength can be approximated by

$$\bar{L} = c\bar{T} \simeq \sqrt{g\bar{h}} \bar{T} . \quad (12)$$

The average period was 10.6 seconds so that

$$L/4 \simeq 5.8 \text{ meters} .$$

The calculations show that the measurement point was near the node of the reflected wave system which would result in relatively small wave heights at the measurement tower.

D. BREAKING WAVE PARAMETERS

Waves tend to arrive at the beach in groups which surfers call "sets". The groups of relatively large waves periodically supply more water, or momentum flux, to the beach and cause a super-elevation or increased set-up inside the surf zone while the group persists. As the last waves

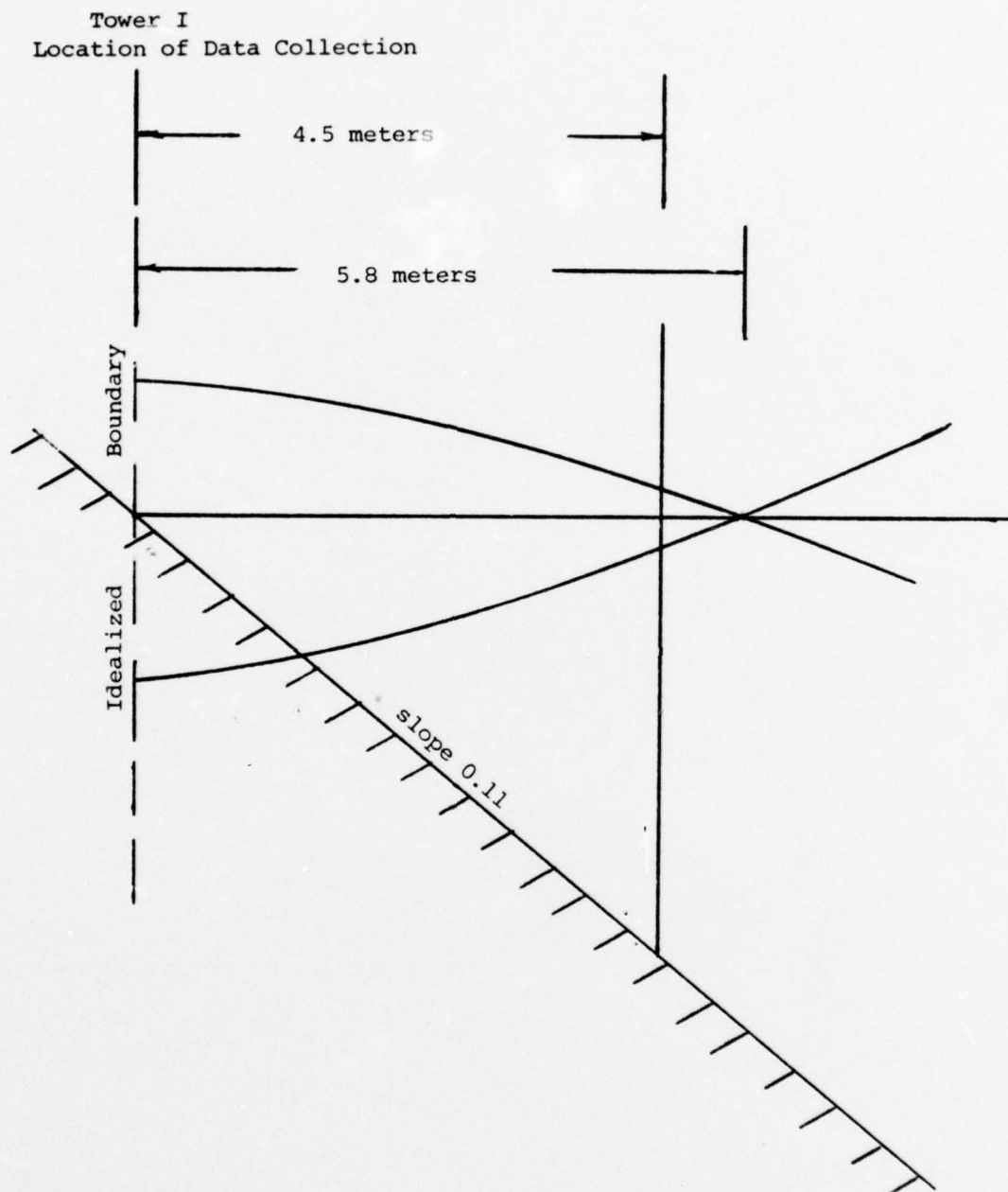


Figure 7. Reflected Wave Node Relation to Gauge Location.

of the group break, the water level begins to fall and remains characteristically low until the next "set" arrives. This periodic rise and fall of the surface elevation is referred to as "surf beat".

A rise in the mean water level was observed to occur shortly after the arrival of a "set" or group of large waves. The amount of deviation of the depth at breaking calculated about the mean value of the depth at breaking, ranged from minus 10.25% to plus 12.28%. This variation in water level is one explanation why waves of such varied sizes could break at essentially the same point in space.

The ratio of breaker height to depth was calculated. This ratio has long been used as a criterion for wave breaking. In other studies the ratio of H_b/h_b has been used over a wide range of bottom and slope conditions in both laboratory and field measurements. The theoretical values range from about 0.73 (Boussinesq, 1871) to 1.03 (Packham, 1952). It is generally found in field work that these are reasonable values.

In 1944 field data were gathered on breaking waves at the Scripps Institution of Oceanography pier (Munk, 1947). This data constitutes a major portion of the relatively few records of breaking waves actually measured in the field. The values of H_b/h_b ranged from 0.67 to 0.82. In this thesis the mean value of the ratio H_b/h_b was found to be 0.86 which is within the range of theoretical values. However, this value is larger than field measurements made by Scripps and smaller than the 0.96 reported by Woods Hole (Gaughan, et al., 1973). The SIO data along with data taken on 10 May 1976 at Carmel River Beach is given in Figure 8. Woods Hole data are not included because no slope information was available. Figure 8 is a plot of H_b versus h_b and contains data from both the SIO report and from this experiment. The values of wave height in

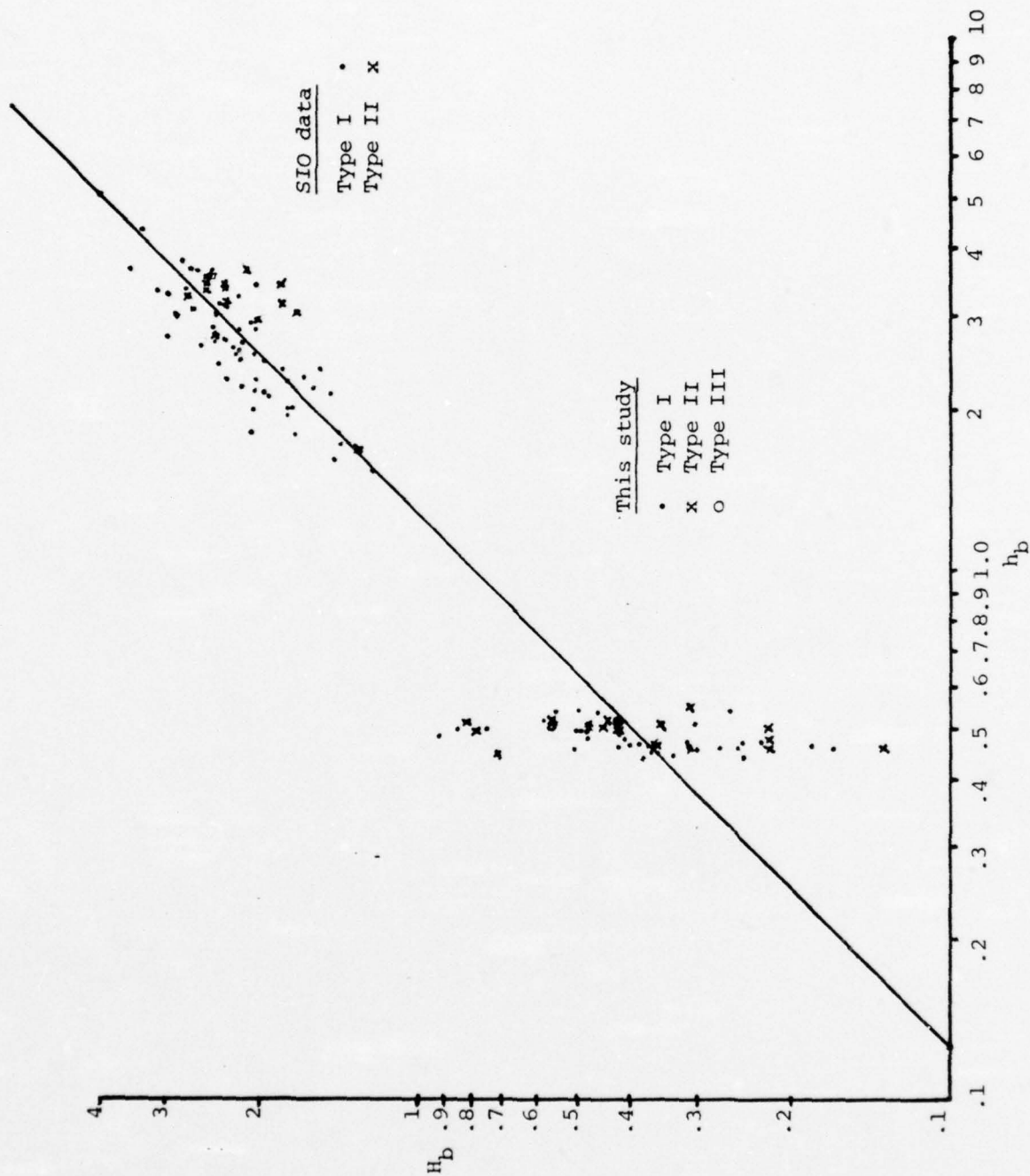


Figure 8. H_b versus h_b for Ocean Breaker Data from the SIO Report of 1949 and This Study.

the SIO data were much larger than those in this report. For reference purposes the theoretical linear slope of 0.78 from solitary wave theory is plotted in the figure.

A comparison between the field data obtained by SIO and this experiment reveals that many individual values of H_b/h_b for the Carmel River Beach were considerably larger in magnitude. The beach slope during the SIO experiments was 0.04 and less while the slope at Carmel River Beach was 0.11. The difference in beach slope presumably accounts for the larger height to depth ratios observed.

The ratio of H_b/L_b was also calculated. The wavelength at breaking, L_b , was determined from the expression relating wavelength to celerity and period,

$$L_b = C_b T_b \quad (13)$$

where wave speed is approximated as,

$$C_b = \sqrt{gh_b} \quad (14)$$

This is a rough approximation to the value of L_b , but from previous work done by Galvin (1975) (where he used two wave towers to measure C_b earlier at this beach) it was found that the above formula slightly overestimated the celerity, again presumably due to a reflected wave system.

The classification of breaker types according to Battjes is shown by the curves in Figure 9. Van Dorn's (1977) data shown in the figure is according to Battjes (1974) reinterpretation of Galvin's (1968) observations. The value of H_b/L_b found in the present study is also plotted in

Breaker Type Symbol

Spilling	Δ	
Plunging	\circ	Galvin (Lab)
	\square	
Collapsing or	\times	Van Dorn (Lab)
Surging	\oplus	This Study (Field)

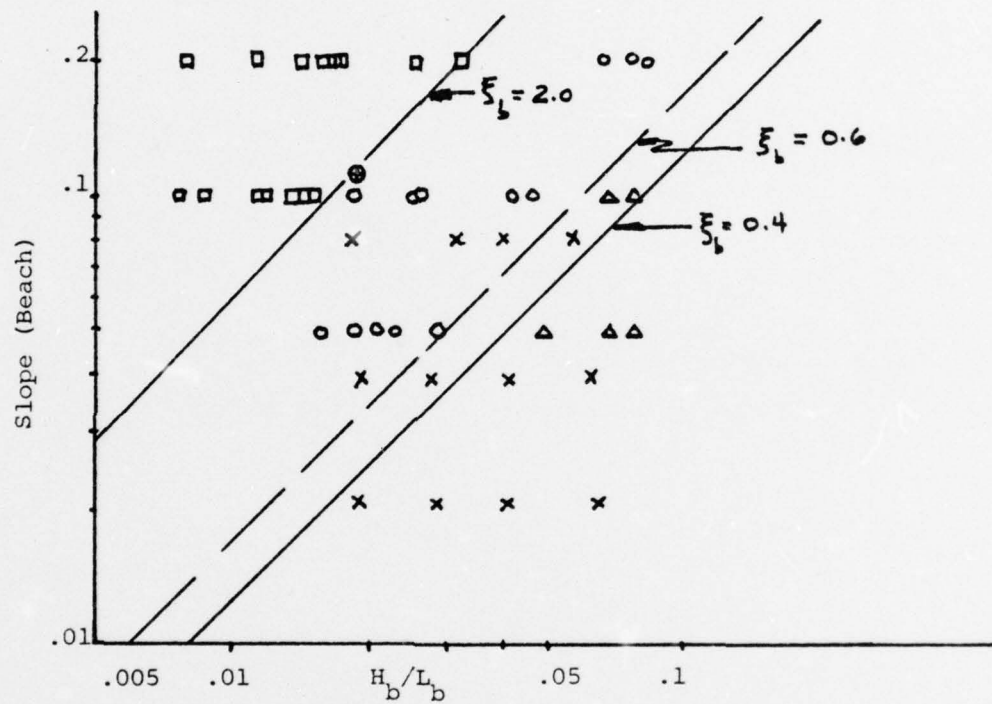


Figure 9. Classification of Present Breaker Types According to Battjes' Reinterpretation of Galvin's Observations.

Figure 9, and indicates that the field evaluation of the breaker type agrees with the Battjes classification.

E. PROBABILITY DISTRIBUTIONS

Probability distributions were plotted for H_b and η_b as shown in Figures 10 and 11, respectively. In each case these distributions at least qualitatively resemble a Rayleigh distribution. Barber (1950) was the first to relate a Rayleigh distribution to the heights of sea waves. Longuet-Higgins (1955) showed theoretically that the distribution of wave height, H , for the case of a narrow banded spectra is given by the Rayleigh distribution,

$$P(H) = \frac{H}{(2\sigma)^2} e^{-(H/2)^2/2\sigma^2} \quad (15)$$

Here we apply the Rayleigh distribution to breaking waves by letting H be the wave height at breaking; σ^2 is the sample variance of the surface profile.

Based on data available at the time (mostly from offshore pressure sensor records) Longuet-Higgins (1952) found a difference between measured and theoretical values for a Rayleigh distribution of only 8% or less. The strict assumptions made in deriving the theoretical probability distribution makes this agreement surprising and it may indicate that the narrowness of the spectrum is not as important as assumed. Since the work by Longuet-Higgins, Koele and deBruyn (1964) and Goodknight and Russel (1963) have found that for deep water waves the goodness of fit value of the Rayleigh distribution is very high. Battjes (1974) also points out that the old dictum proposed by Rayleigh himself,

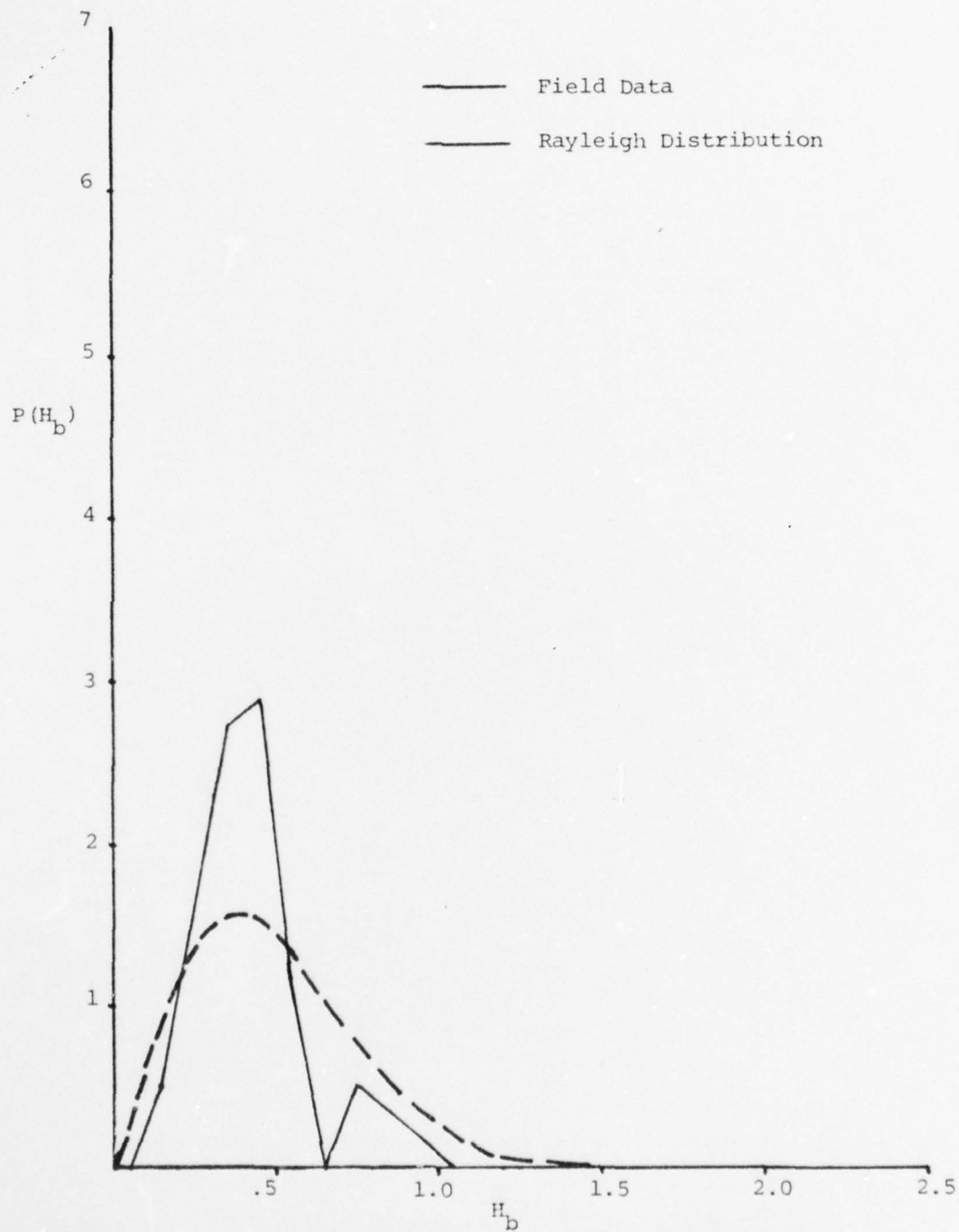


Figure 10. Probability Distribution of Wave Heights and Corresponding Theoretical Rayleigh Distribution.

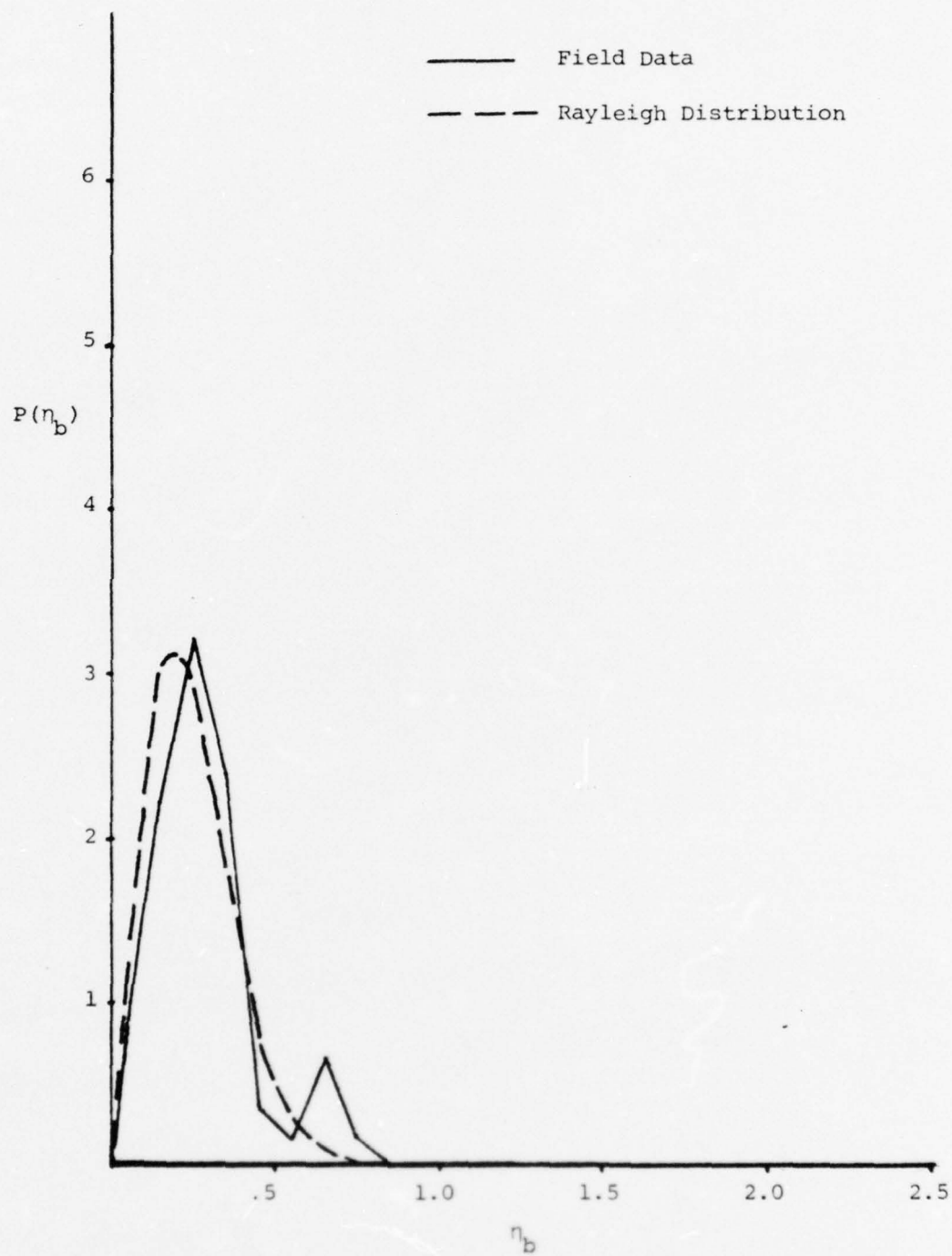


Figure 11. Probability Distribution of Wave Amplitudes and Corresponding Theoretical Rayleigh Distribution.

"The basic law of the seaway is the apparent lack of any law," seems somewhat in doubt based on these findings.

The following explanation is given by Battjes (1974) as the reason why wave heights are to a good approximation Rayleigh distributed even for waves that are non-linear such as at breaking and do not possess a narrow spectrum. Even though breaking waves have higher crests and shallower troughs, the increase in crest compensates for the shallowing of the trough and H values remain essentially unchanged. Taking the definition for crest elevation as being the greatest elevation between successive zero-crossings, it was assumed that the crest elevation correlates strongly with the immediately following largest trough depth between successive zero-crossings. Battjes observed that Jahns and Wheller (1972) reject this assumption. They point out that for a wide spectrum a relatively high crest is on the average followed by a trough that is not relatively deep. They argue that application of a Rayleigh distribution would lead to an overestimation of the probability of exceeding some arbitrary value for the relatively high waves if the spectrum were not narrow.

It was found in the Carmel River Beach data that the Rayleigh distribution generally tends to underestimate the probability of exceeding some arbitrary value of η_b and overestimates the probability of exceedence for values of H_b . This result tends to agree with Jahns and Wheller's argument.

The variance used in calculating the Rayleigh distribution was derived from the total record of instantaneous water level whereas the breaking wave height data only includes those waves that broke on the tower. Hence, the calculated variance leads to an overestimation of the probability of the wave height exceeding some arbitrary value.

Probability distributions were also calculated for horizontal water particle velocities measured under the breaking waves, and are shown in Figure 12. Distributions were calculated for motion in both directions, i.e., seaward and shoreward. These were compared to the Rayleigh distribution, but it was found that the probability of exceeding some arbitrary value is considerably underestimated.

The distributions of the velocities in the seaward direction are strongly negatively skewed showing more large maximum velocities than small values. The shoreward velocities are negatively skewed but not to the same degree as the seaward. The larger seaward velocities would be expected on a steep beach because the seaward velocity is the sum of backwash due to the force of gravity plus the particle velocity in the trough of the wave. The Rayleigh distribution is positively skewed and therefore does not represent the distribution of the observed velocities.

The probability distributions for the ratio of $V_{\max}^{(+)} / C_b$ for both collapsing and plunging breakers, shown in Figure 13, indicate that waves break over the range of values from 0.5 to 1.5. The kinematic criteria states that breaking will occur when $V \geq C_b$ (Table I). The breakers that occurred for values of $V_{\max}^{(+)} / C_b < 1.0$ indicate that other processes may control breaking, such as the water deficit mentioned earlier. Figure 14 is a composite of all the V_{\max} / C_b ratios computed on 10 May 1976.

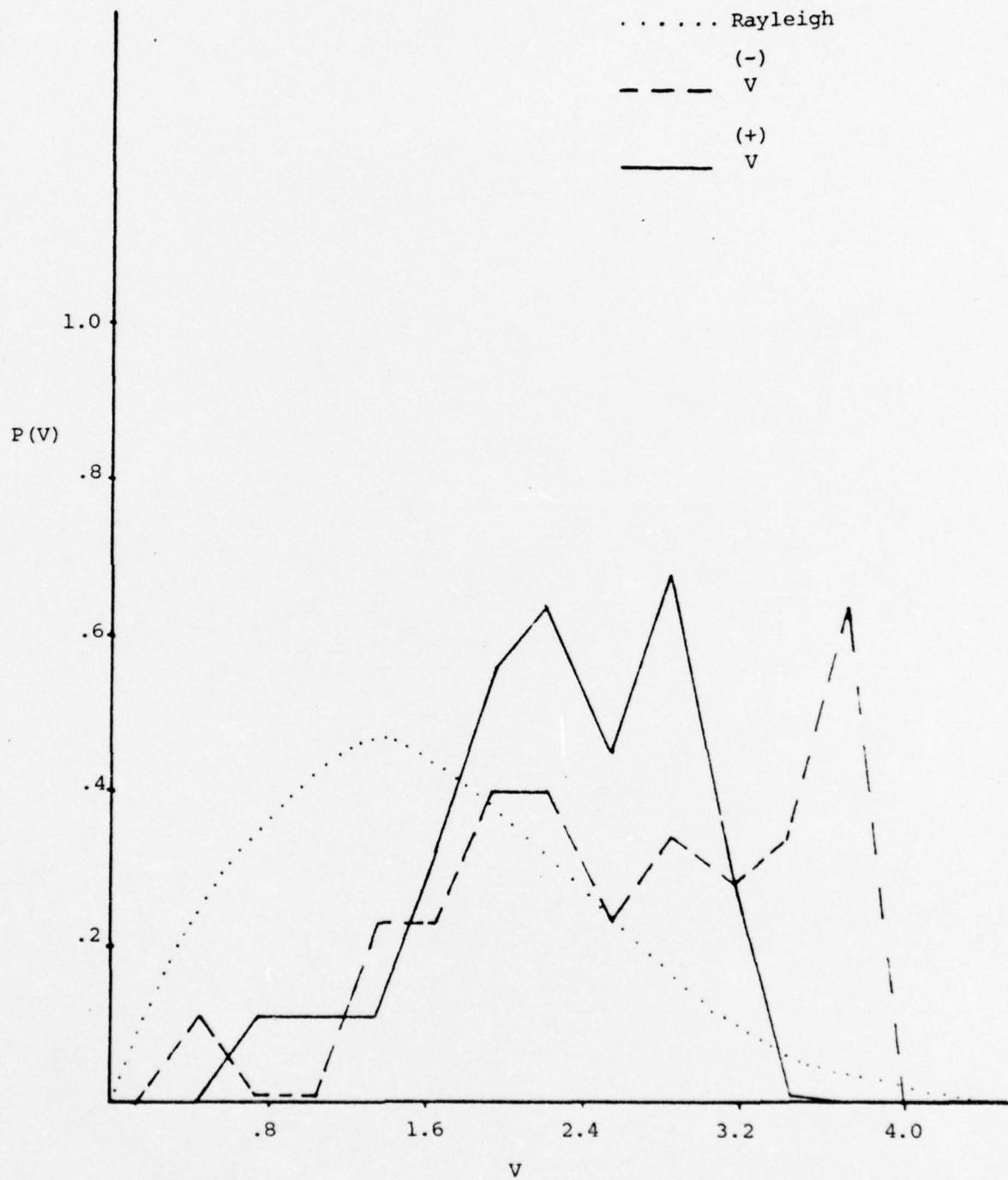


Figure 12. Probability Distribution of Shoreward Horizontal Velocity under a Breaking Wave, Seaward Swash Velocity and Corresponding Theoretical Rayleigh Distribution.

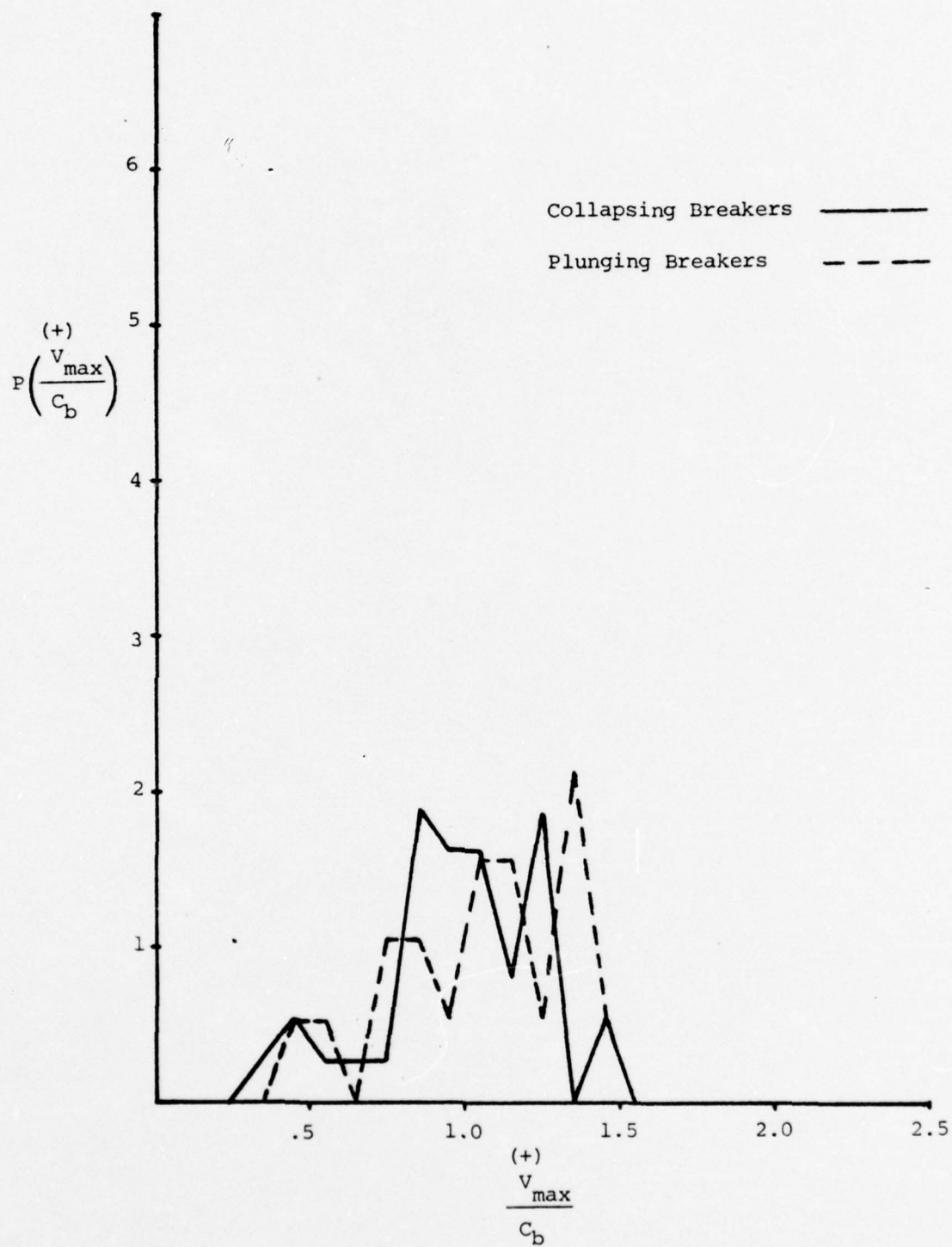


Figure 13. Probability Distribution of $\frac{v_{\max}}{c_b}$ for Collapsing and Plunging Breakers.

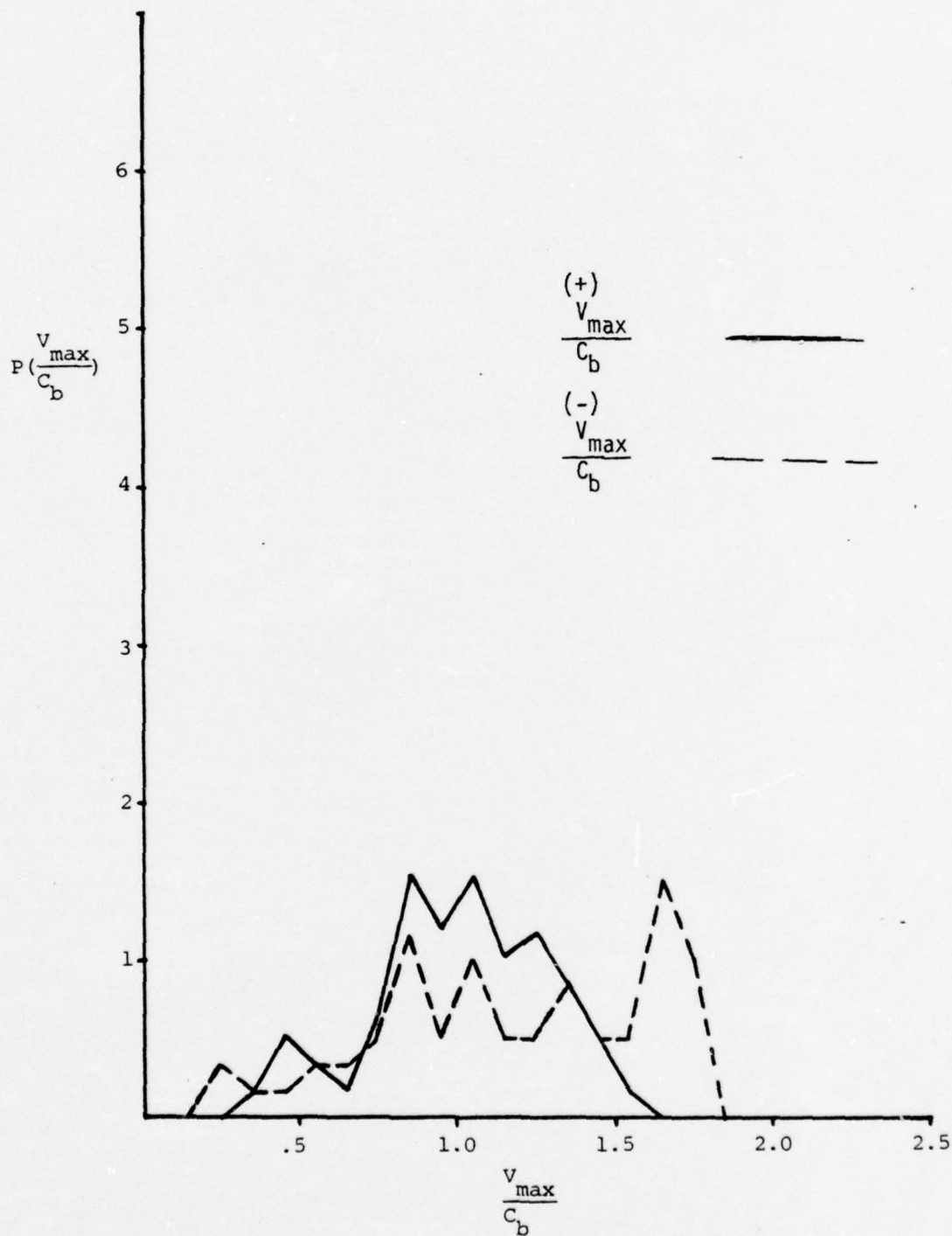


Figure 14. Probability Distribution of V_{\max}/C_b for Composite of All Breakers Measured in This Study.

V. CONCLUSIONS

The following conclusions are derived from the field measurements made on Carmel River Beach on 10 May 1976. The predominate breaker types were collapsing and plunging. The beach slope was 0.11 indicating a steep slope.

1. Very little difference between the ratio of H_b/h_b for the various breaker types was measured.
2. The mean ratio of H_b/h_b calculated from the data was 0.86 and is close to generally accepted theoretical values.
3. Breaking wave distributions of H_b and η_b are qualitatively described by the Rayleigh distribution. The probability of exceedance is overestimated in the case of H_b and underestimated in the case of η_b .
4. Distribution of the onshore and offshore water particle velocities in breaking waves is negatively skewed and therefore not described by the Rayleigh distribution.
5. The mean value of the wave height at breaking may, in the case of reflected waves, be less than the initial deep water wave height. This will only occur close to a nodal point.
6. The value of the ratio of $V_{\max}^{(+)} / C_b$ was computed for all the waves that broke on the tower and in many cases the ratio was less than 1.0. This was most prominent for the collapsing breakers. Since the kinematic breaking criterion states that $V_{\max} \geq C_b$ at breaking, backwash and wave reflection must be important in describing breaking criterion on steep beaches.

7. The breaking mechanism in collapsing breakers appears to be the turbulence present in the base of the wave caused by a water deficit in the swash zone.

APPENDIX A

The calibration of the wave gauge along with its associated linearizing circuit was carried out in the NPS physics laboratory deep acoustics tank. Figure 15 shows a calibration plot for wave gauges.

CALM is the slope of the curve in Figure 15 in meters/volt

CALA = height of gauge above bottom related to the intercept of the curve.

The Engineering Physics Company water current meter was calibrated by oscillating it in a water tank, as described by Steer (1972). Steer obtained a calibration factor of 0.610 meters/sec/volt for the probe used in this experiment.

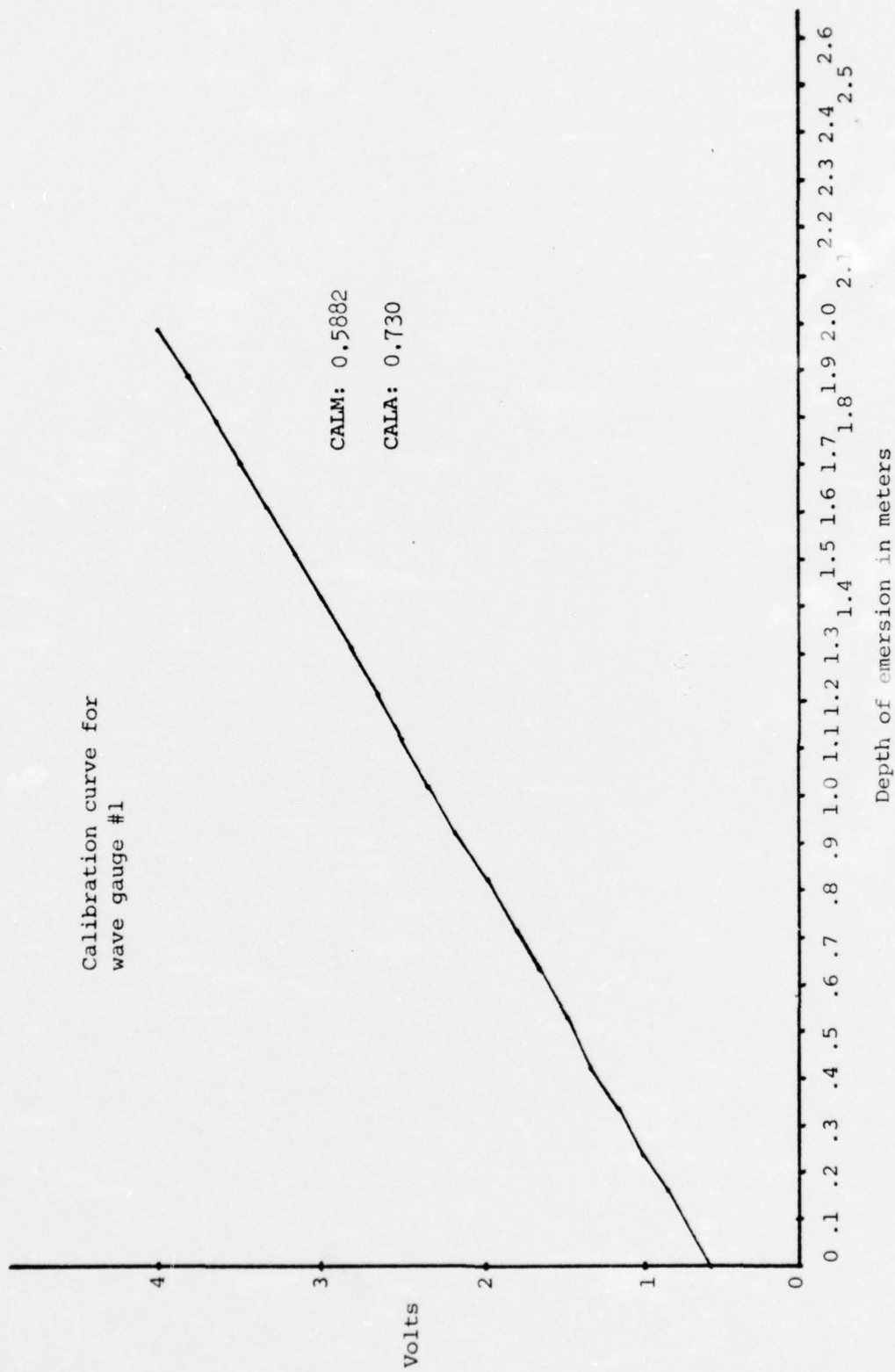


Figure 15. Calibration Curve for the Wave Gauge Used in This Experiment.

APPENDIX B

This appendix contains a collection of probability distributions
for H_b/h_b , H_b , η_b , V , V , and V_{\max}/C_b .
(+) (-) (-)

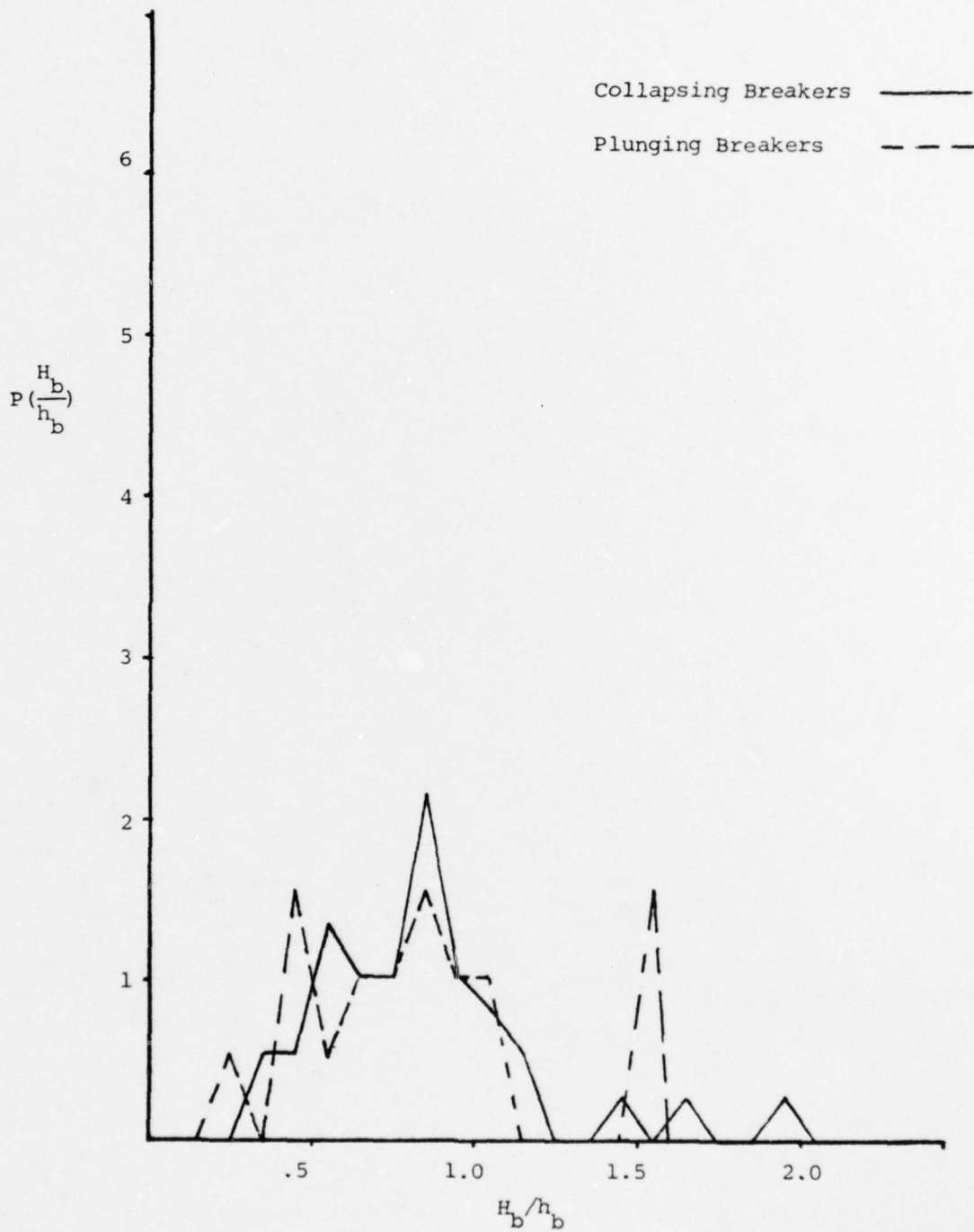


Figure 16. Probability Distribution of H_b/h_b for Collapsing and Plunging Breakers.

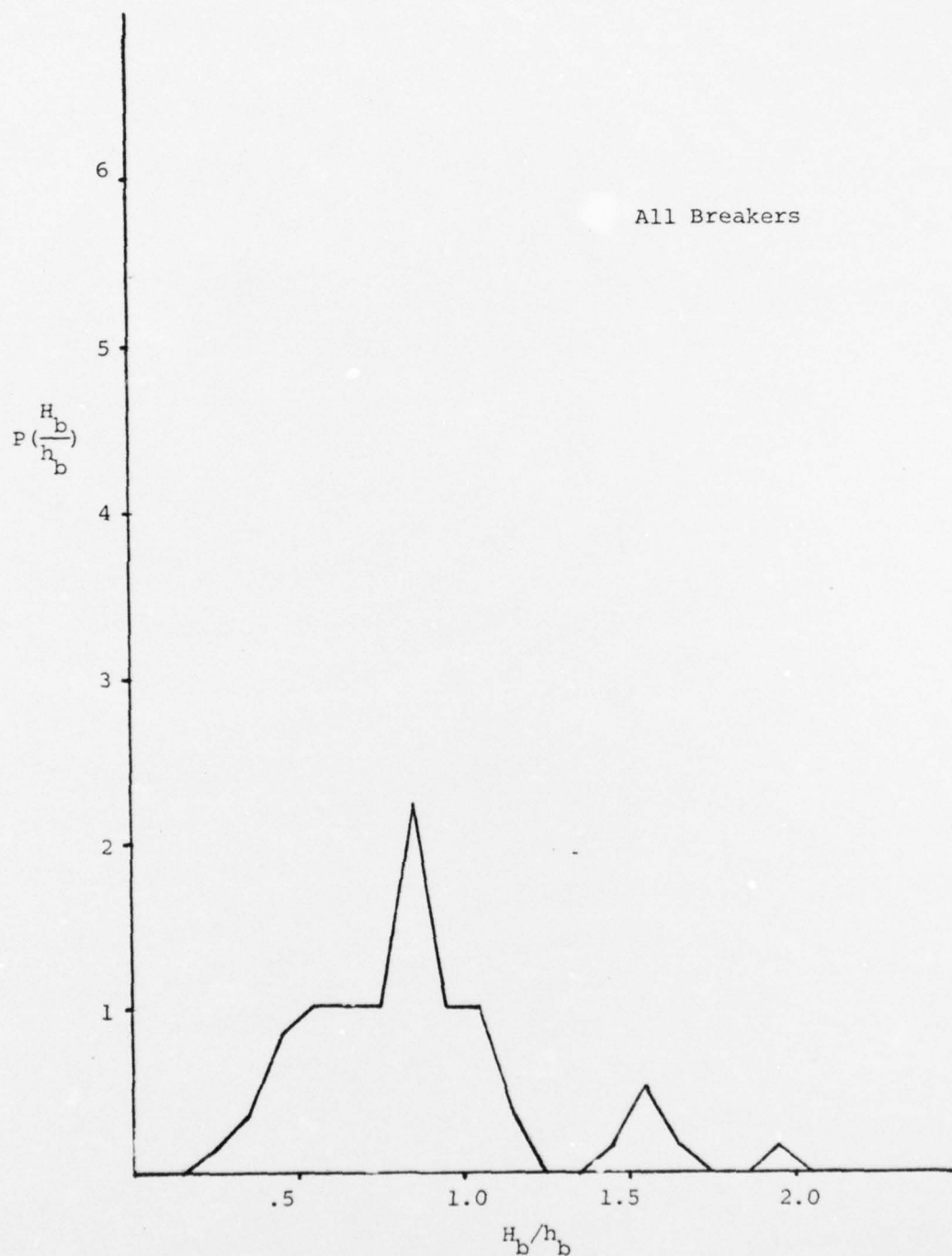


Figure 17. Probability Distribution of H_b/h_b for Composite of All Waves on 10 May 1976.

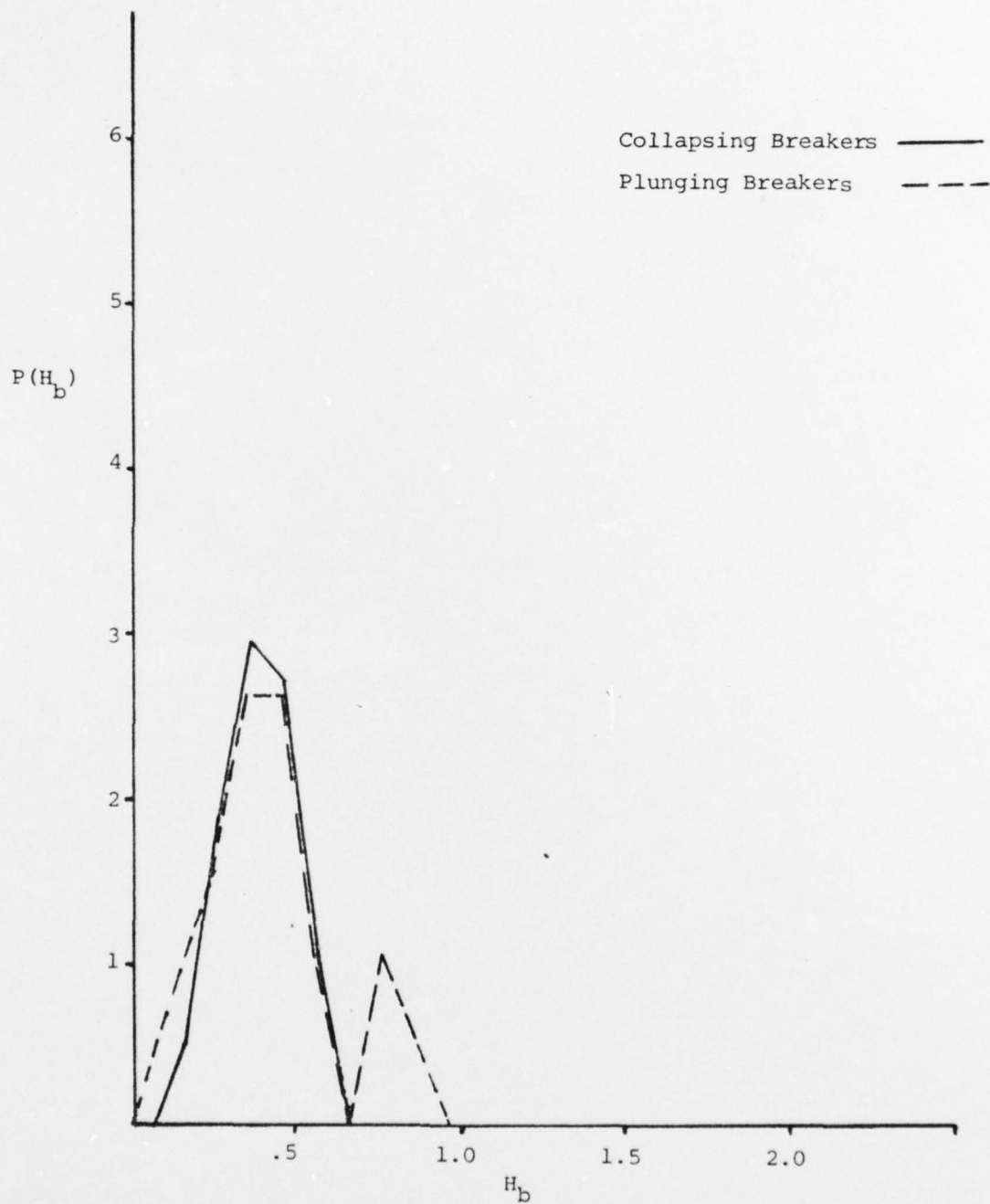


Figure 18. Probability Distribution of H_b for Collapsing and Plunging Breakers.

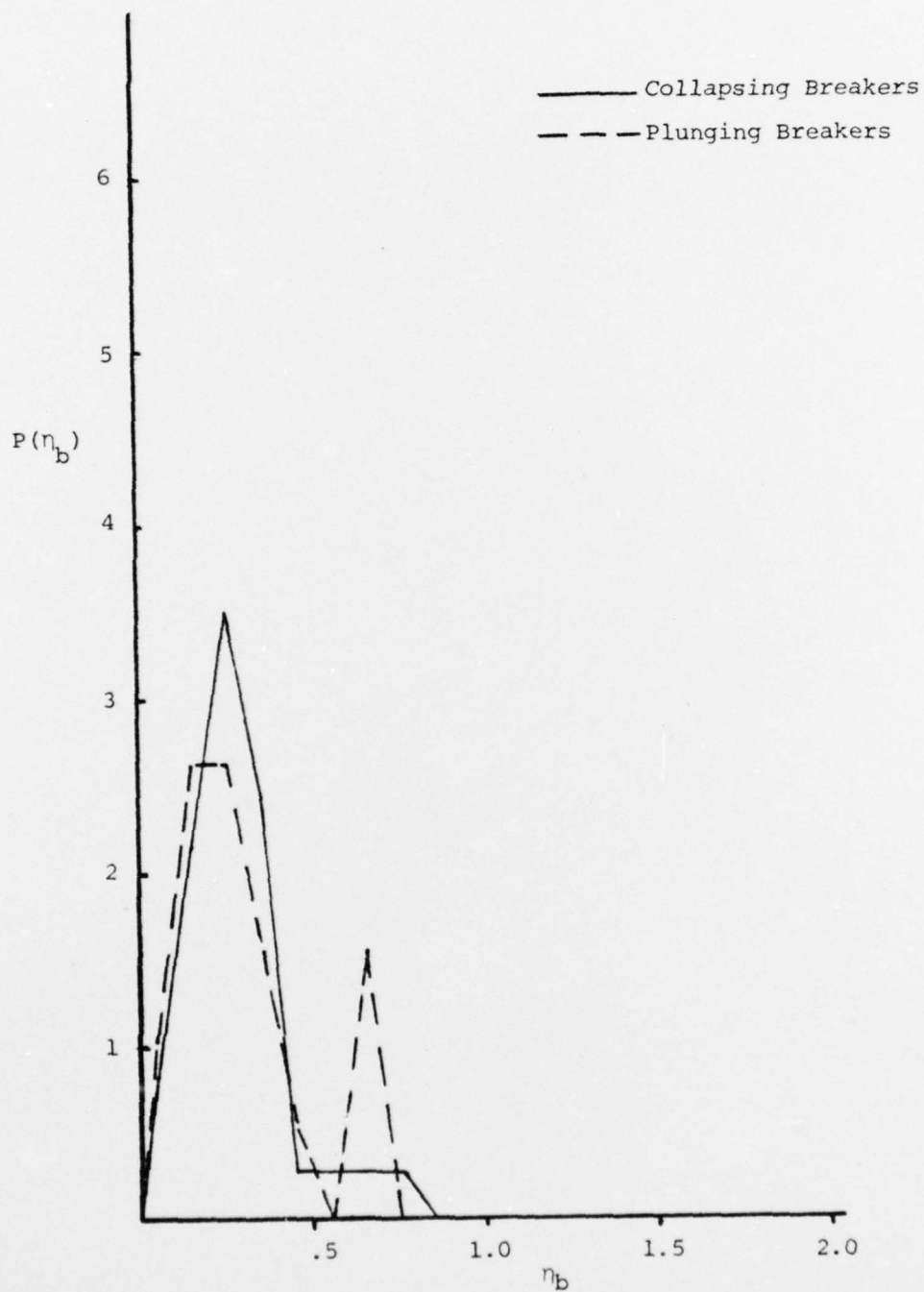


Figure 19. Probability Distribution of η_b for Collapsing and Plunging Breakers.

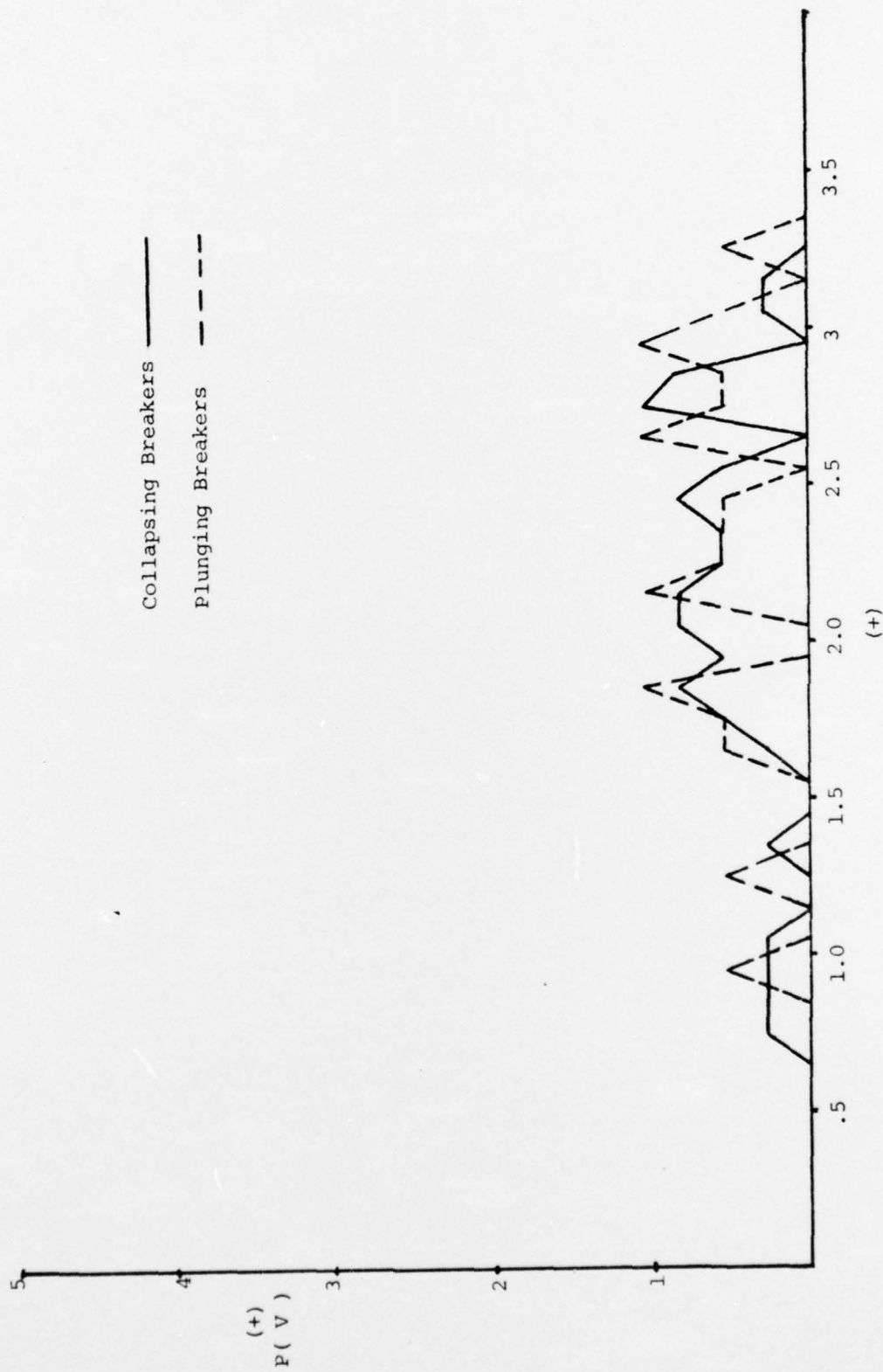


Figure 20. Probability Distribution of V for Collapsing and Plunging Breakers.

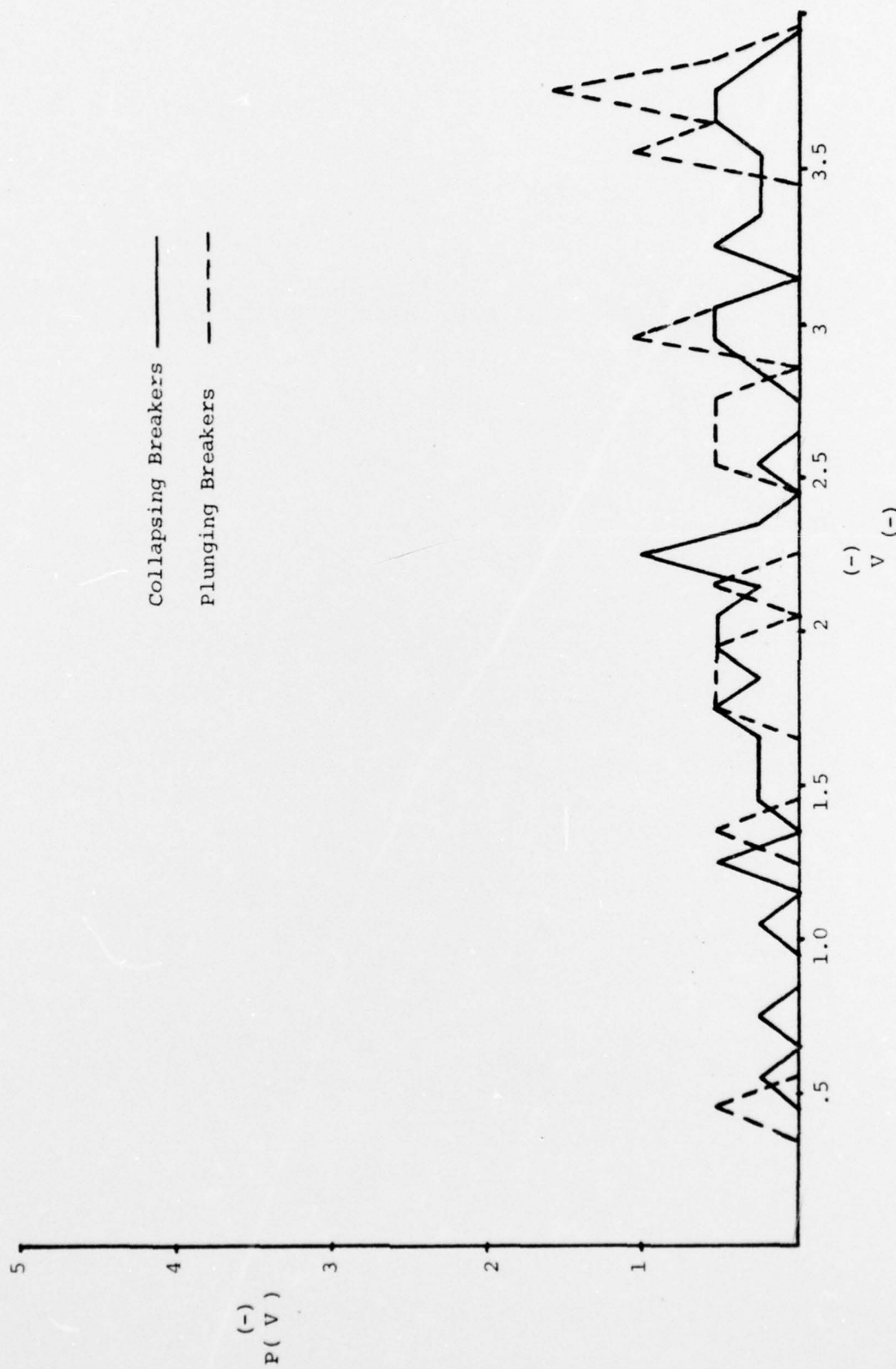


Figure 21. Probability Distribution of V for Collapsing and Plunging Breakers.

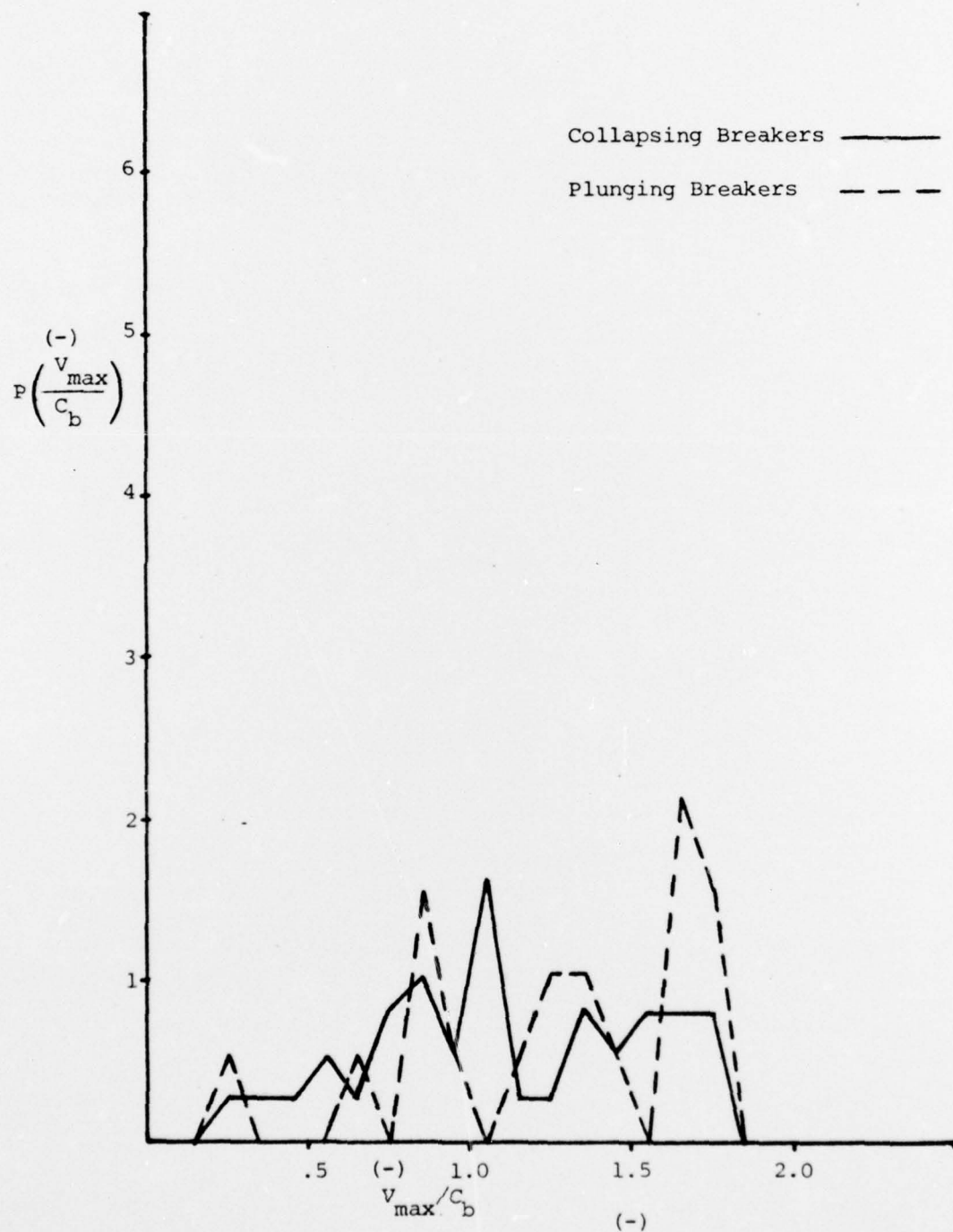


Figure 22. Probability Distribution of $\frac{V_{\max}}{C_b}$ for Collapsing and Plunging Breakers.

APPENDIX C

This appendix consists of a table containing the data collected during the Carmel River Beach experiment on 10 May 1976. The table contains all the data taken directly from the plots as well as some ratios computed from these data. For these data, $m = 0.11$ and $H'_O = 0.49$ meters.

Wave Parameters Measured or Computed
During Carmel River Beach (Thornton-Hultstrand)
Wave Type: 1 Collapsing 2 Plunging 3 Spilling

Wave Type	Hb (M)	η_b (M)	hb (M)	Hb/L _b	(+) Vmax/Cb	(-) Vmax/Cb	+V _H =upbeach	-V _H =downbeach
1	.3000	.1940	.4600	.6522	1.442	1.049	3.16	2.30
1	.2500	.1400	.4600	.5435	.967	1.026	2.12	2.25
1	.5140	.4000	.4600	1.1174	1.296	1.163	2.84	2.55
1	.4220	.3240	.4620	.9134	1.099	.762	2.41	1.67
2	.1340	.0260	.4680	.2863	1.323	1.255	2.90	2.75
1	.1820	.0600	.4680	.3889	.502	1.665	1.10	3.65
2	.2200	.1060	.4640	.4741	1.186	.616	2.60	1.35
2	.3600	.2480	.4620	.7792	1.022	1.414	2.24	3.10
1	.2760	.1800	.4600	.6000	.411	.575	.90	1.26
1	.3660	.2680	.4560	.8026	1.268	.867	2.78	1.90
1	.1660	.1000	.4600	.3609	.319	.274	.70	.60
1	.3800	.2800	.4400	.8636	.844	1.565	1.85	3.43
1	.2460	.1540	.4400	.5591	.821	.821	1.80	1.80
1	.3320	.2280	.4460	.7444	1.095	1.004	2.40	2.20
1	.3540	.2620	.4520	.7832	.844	.479	1.85	1.05
2	.7100	.6060	.4500	1.5778	.867	1.734	1.90	3.80
2	.3140	.1880	.4740	.6624	.985	.862	2.16	1.89
2	.3620	.2340	.4760	.7605	1.200	1.145	2.63	2.51

Wave Parameters (Continued)

1	.2480	.1240	.4720	.5254	1.277	1.405	2.80	3.08
1	.3140	.2000	.4740	.6624	.890	.926	1.95	2.03
1	.4100	.2800	.4760	.8613	1.049	1.391	2.30	3.05
2	.2260	.1000	.4800	.4708	.748	.817	1.64	1.79
1	.2280	.1040	.4740	.4810	1.186	.798	2.60	1.75
1	.4000	.2860	.4680	.8547	.734	1.049	1.61	2.30
1	.3140	.2240	.4680	.6709	1.168	1.063	2.56	2.33
1	.3700	.2520	.4640	.7974	1.118	1.711	2.45	3.75
1	.3840	.2600	.4720	.8136	1.305	.931	2.86	2.04
1	.4840	.3640	.4760	1.0168	1.036	1.688	2.27	3.70
1	.9200	.7820	.4820	1.9087	.812	1.642	1.78	3.60
2	.2200	.1280	.5040	.4365	.844	1.341	1.85	2.94
2	.4220	.2740	.4940	.8543	1.483	1.642	3.25	3.60
1	.4800	.3300	.4960	.9677	.867	1.537	1.90	3.37
1	.5800	.4040	.5200	1.1154	1.277	1.505	2.80	3.30
1	.4660	.2800	.5400	.8630	.958	1.282	2.10	2.81
1	.5000	.3040	.5420	.9225	1.099	.876	2.41	1.92
1	.4300	.2800	.5500	.7818	.620	.589	1.36	1.29
2	.4800	.3120	.5180	.9266	1.382	1.218	3.03	2.67
2	.4800	.3200	.5060	.9486	1.346	1.711	2.95	3.75
1	.8480	.6960	.5000	1.6960	.871	.899	1.91	1.97
2	.4520	.2900	.5060	.8933	1.255	1.679	2.75	3.68
2	.5600	.4000	.5160	1.0980	.798	.899	1.75	1.97
2	.4380	.2620	.5160	.8488	1.369	1.369	3.00	3.00

Wave Parameters (Continued)

3	.4200	.2520	.5140	.8171	.798	1.688	1.75	3.70
1	.4900	.3960	.4960	.9879	.981	.703	2.15	1.54
1	.5080	.3540	.4980	1.0201	1.081	1.341	2.37	2.94
1	.4260	.3800	.4900	.8694	.949	1.492	2.08	3.27
2	.7780	.6380	.4960	1.5685	1.118	1.624	2.45	3.56
1	.3480	.1800	.5000	.6960	.976	1.779	2.14	3.90
1	.7460	.5860	.5000	1.4920	1.296	1.734	2.84	3.80
2	.5600	.3960	.5160	1.0853	.456	1.779	1.00	3.90
2	.8200	.6420	.5200	1.5769	1.095	1.697	2.40	3.72
1	.5520	.3500	.5420	1.0185	1.414	1.346	3.10	2.95
2	.3160	.1140	.5500	.5745	1.004	.976	2.20	2.14
1	.2600	.0660	.5460	.4762	.931	.365	2.04	0.80
3	.2460	.2400	.5240	.8130	1.578	1.186	3.46	2.60
1	.2460	.2860	.5260	.8783	1.277	1.026	2.80	2.25
3	.5580	.3860	.5140	1.0856	1.328	1.610	2.91	3.53
1	.3020	.2100	.5140	.5875	.433	.661	0.95	1.45
2	.3500	.2000	.5100	.6863	.570	.219	1.25	0.48

REFERENCES

- Bendat, J. S., and A. G. Piersol, 1966. Measurement and Analysis of Random Data. Wiley, p. 123-142.
- Bowen, A. J., D. L. Inman, and V. P. Simmons, 1968. Wave set-down and set-up. *Journal of Geophysical Research* 73(8): 2569-2577.
- Dean, R. G., 1968. Breaking wave criteria: a study employing numerical wave theory. In: *Proceedings Eleventh Conference Coastal Engineering*. 1: 108-123.
- Department of the Army, Corps of Engineers, 1973. Shore Protection Manual, v. 1.
- Galvin, C. J., 1968. Breaker type classification on three laboratory beaches. *Journal of Geophysical Research* 73(12): 3651-3659.
- Galvin, C. J., 1972. Waves breaking in shallow water. In: *Waves on beaches and resulting sediment transport*. Ed. R. E. Meyer. London Academic Press, p. 413-456.
- Galvin, J. J., 1975. Kinematics of Surf Zone Breaking Waves: Measurement and Analysis, M.S. Thesis, Naval Postgraduate School, Monterey.
- Gaughan, M. K., and P. D. Komar, 1975. The theory of wave propagation in water of gradually varying depth and the prediction of breaker type and height. *Journal of Geophysical Research* 80(21): 2991-2996.
- Kinsman, B., 1965. Wind Waves. Prentice-Hall, Inc., p. 325-352, 427-483.
- Munk, W. H., and M. Winbush, 1969. A rule of thumb for wave breaking over sloping beaches. *Oceanology* 9: 56-59.
- Munk, W. H., 1949. The Solitary Wave Theory and Its Application to Surface Problems. *Annals of the New York Academy of Science*, v. 51, p. 376-424.
- Oregon State University, School of Oceanography, Ref. 73-12, 1973. Breaking Waves: A Review of Theory and Measurements, Gaughan, M. K., P. D. Komar, and J. H. Nath.
- Pierson, W. J., Jr., Neumann, Gerhard, and R. W. Jones, 1971. Observing and Forecasting Ocean Waves. H. O. Publication 603, p. 32-40.
- Price, R. K., 1970. Detailed structure of the breaking wave. *Journal of Geophysical Research* 75(27): 5276-5278.

- Price, R. K., 1970. The breaking of water waves. *Journal of Geophysical Research* 76(6): 1576-1581.
- Smith, R. M., 1976. Breaking Wave Criteria on a Sloping Beach, M.S. Thesis, Naval Postgraduate School, Monterey.
- Steer, R., 1972. Kinematics of Water Particle Motion Within the Surf Zone, M.S. Thesis, Naval Postgraduate School, Monterey.
- Thornton, E. B., 1969. Longshore Current and Sediment Transport. Department of Coastal and Oceanographic Engineering Report 5.
- Weggel, A. M., 1972. Maximum breaker height. *Journal of Waterways, Harbors and Coastal Engineering Division*. In: Proceedings of American Society of Civil Engineers, U. S. Army Coastal Engineering Research Center reprint. 3-73: 529-548.
- Wiegel, R. L., 1964. Oceanographical Engineering. Prentice Hall, Inc., p. 11-74, 150-178.

INITIAL DISTRIBUTION LIST

	No. Copies
1. Defense Documentation Center Cameron Station Alexandria, Virginia	2
2. Library, (Code 0142) Naval Postgraduate School Monterey, California 93940	2
3. Department Chairman, Code 68 Department of Oceanography Naval Postgraduate School Monterey, California 93940	3
4. Assoc. Professor E. B. Thornton, Code 68 Department of Oceanography Naval Postgraduate School Monterey, California 93940	5
5. Assoc. Professor J. J. von Schwind, Code 68 Department of Oceanography Naval Postgraduate School Monterey, California 93940	1
6. Oceanographer of the Navy Hoffman Building No. 2 200 Stovall Street Alexandria, Virginia 22332	1
7. Office of Naval Research Code 462 Arlington, Virginia 22217	1
8. Dr. Robert E. Stevenson Scientific Liaison Office, ONR Scripps Institution of Oceanography La Jolla, California 92037	1
9. Library, Code 3330 Naval Oceanographic Office, NSTL Bay St. Louis, Mississippi 29522	1
10. Professor Warren C. Thompson, Code 68 Department of Oceanography Naval Postgraduate School Monterey, California 93940	1

- | | | |
|-----|--|---|
| 11. | SIO Library
University of California, San Diego
La Jolla, California 92037 | 1 |
| 12. | Department of Oceanography Library
University of Washington
Seattle, Washington 98105 | 1 |
| 13. | Department of Oceanography Library
Oregon State University
Corvallis, Oregon 97331 | 1 |
| 14. | Commanding Officer
Fleet Numerical Weather Central
Monterey, California 93940 | 1 |
| 15. | Department of the Navy
Commander Oceanographic System Pacific
Box 1390
FPO San Francisco 96610 | 1 |
| 16. | Commanding Officer
Naval Environmental Prediction Research Facility
Monterey, California 93940 | 1 |
| 17. | Lt. Richard M. Smith
c/o 8245 Van Noord Avenue
North Hollywood, California 91605 | 1 |
| 18. | Commander Naval Weather Service Command
Naval Weather Service Headquarters
Washington Navy Yard
Washington, D. C. 20390 | 1 |
| 19. | Coastal Studies Institute
Louisiana State University
Baton Rouge, Louisiana 70803 | 1 |
| 20. | School of Marine and Atmospheric Science
University of Miami
Miami, Florida 33149 | 1 |
| 21. | Lt. Victor S. Hultstrand
NAVOCEANO, NSTL
Bay St. Louis, Mississippi 39522 | 5 |

FILMED
6-17

